UNIVERSITY OF CALIFORNIA, BERKELEY

PROFESSIONAL REPORT

Interactions of flooding events, demand of services, and accessibility: a network science approach

Author:
Andrew H. G. NELSON

Supervisor:
Prof. Marta C. GONZALEZ

A professional report submitted in fulfillment of the requirements for the degree of Master of City Planning

in the

Department of City and Regional Planning

December 24, 2019

Declaration of Authorship

I, Andrew H. G. NELSON, declare that this professional report titled, “Interactions of flooding events, demand of services, and accessibility: a network science approach” and the work presented in it are my own. I confirm that:

- This work was done wholly or mainly while in candidature for a research degree at this University.
- Where any part of this professional report has previously been submitted for a degree or any other qualification at this University or any other institution, this has been clearly stated.
- Where I have consulted the published work of others, this is always clearly attributed.
- Where I have quoted from the work of others, the source is always given. With the exception of such quotations, this professional report is entirely my own work.
- I have acknowledged all main sources of help.
- Where the professional report is based on work done by myself jointly with others, I have made clear exactly what was done by others and what I have contributed myself.

Signed:

Date:

"We must face up to an inescapable reality: the challenges of sustainability simply overwhelm the adequacy of our responses. With some honorable exceptions, our responses are too few, too little, and too late."

Kofi Annan

UNIVERSITY OF CALIFORNIA, BERKELEY

Abstract

Marta C. Gonzalez
Department of City and Regional Planning

Master of City Planning

Interactions of flooding events, demand of services, and accessibility: a network science approach

by Andrew H. G. NELSON

In developing nations, incorporating vulnerability measures into existing urban transportation plans to maximize co-benefits of investments is a powerful way to decide on infrastructure investments. In particular, the interactions between transportation networks, climate, and the access to services have not been widely explored. This study proposes a method to identify how we can measure the interactions of accessibility, service demand, and climate vulnerability at the street level. We propose a network metric, Service Centrality (SC), to classify the importance in accessibility to critical services, and combine it with its vulnerability to climate events. To that end, we incorporate a method that generates flooding scenarios. We present a case study in Freetown, Sierra Leone to demonstrate how it can be used to inform the impact of possible capacity-building or hardening interventions. We demonstrate how major flooding hazards create demand and accessibility shifts for services, based on the distribution of facilities. Positive SC shifts under hazard conditions represent an increase in importance to the network system in facility demand and access. We use seasonal flooding hazards to show that neighborhoods within a single service area differently affected by expected precipitation levels. We also show how governments and institutions may use this methodology in planning by exploring its application to transit systems and considering interactions with the uneven geographic distribution of poverty. Taken together, we present a framework to estimate the benefits of investments in road infrastructures that takes into account travel demand and accessibility to target facility types such as schools and hospitals.

Acknowledgements

The author expresses his sincere thanks to Prof. Marta Gonzalez for her dedicated education, advisement, and support through a long and complex project. The last two years would not have had nearly the same eye-opening impact without her.

The author thanks the faculty of the Departments of City Planning and Civil Engineering for grounding his research in theory and practice. The author thanks Xavier Espinet Alegre, Fatima Arroyo Arroyo, and Dunstan Matekenya of the World Bank for their invaluable assistance in providing data, advice, and connection to the government and people of Sierra Leone. Finally, the author thanks Sarah Lindbergh, Lucy Stephenson, and Jeremy Halpern for working together on the project and publication which inspired the continuation of this work.

Contents

List of Figures

List of Tables

List of Abbreviations

ASTER	**A**dvanced **S**paceborn **T**hermal **E**mission (and) **R**eflection
BC^{aug}	**B**etweenness **C**entrality, **aug**mented
CBD	**C**entral **B**usiness **D**istrict
CDR	**C**all **D**etail **R**ecords
CN	**C**urve **N**umber
DEM	**D**igital **E**levation **M**odel
EA	**E**numeration **A**rea
GIS	**G**eographic **I**nformation **S**ystem
GTFS	**G**eneral **T**ransit **F**eed **S**pecification
HEC-HMS	**H**ydrologic **E**ngineering **C**enter's **H**ydrologic **M**odeling **S**ystem
HEC-RAS	**H**ydrologic **E**ngineering **C**enter's **R**iver **A**nalysis **S**ystem
HOT	**H**umanitarian **O**penStreetMap **T**eam
LIDAR	**Li**ght **D**etection **a**nd **R**anging
METI	**M**inistry (of) **E**conomy, **T**rade, (and) **I**ndustry (of Japan)
NASA	**N**ational **A**eronautics (and) **S**pace **A**dministration
OD	**O**rigin-**D**estination
OSM	**O**pen**S**treet**M**ap
SC	**S**ervice **C**entrality
TIN	**T**riangular **I**rregular **N**etworks
USGS	**U**nited **S**tates **G**eological **S**urvey

List of Symbols

v	network edge
σ_{ij}	the distance-weighted Dijkstra's shortest path between unordered node pairs i and j
σ_{kl}	the distance-weighted Dijkstra's shortest path between the road network node closest to the centroid of neighborhood k and the road network node closest to the facility l nearest to k
NF	matrix assigning population values for neighborhood k to closest facility l
OD	trips measured in an origin-destination matrix

Dedicated to the victims of the Regent-Lumley Landslide of August 14, 2017

Chapter 1

Introduction

1.1 Background

Prioritizing climate resilience in a developing nation presents important challenges, particularly when rebuilding following a disaster or other major service disruption. The high complexity of urban systems increases the ability for intertwined functions to be disrupted by single events (Graham, 2012), emphasizing the importance of estimating vulnerability to shocks. Increased physical vulnerability to shocks compounds when considered with systemic vulnerabilities in other societal sectors (World Bank Group, 2018; Pelling et al., 2004; Rosenzweig et al., 2018). Conversely, catastrophes may be perceived as opportunities for innovation by identifying what enhances the capacities of social systems to deal with threats more competently, particularly by identifying co-benefits of improvements to multiple systems (Keck and Sakdapolrak, 2013).

In a previous work (Nelson et al., 2019), we examined the city of Freetown, Sierra Leone in the aftermath of a devastating flooding and mudslide event, the Regent-Lumley Disaster of 2017. In addition to loss of life and property, the effects of the mudslide on the urban transportation network were severe, bisecting the city by disabling several key bridges. While the previous study helped focus ongoing reconstruction efforts for the transportation system by using network analysis to identify road network nodes which intersected with areas of high climate risk, it lacked consideration of the co-benefits which is introduced by considering the interaction of the road network with facility accessibility and population demand.

1.2 Road Networks

Accessibility analysis and facility demand analysis widely depend upon the transportation system's representation as a mathematical network - nodes, connected by links (Kurant and Thiran, 2006; Buhl et al., 2006; Cardillo et al., 2006) - to estimate the distances from facilities to the populations they serve. While network science has its origins in social science, it has been applied to numerous fields that deal with interdependent complex systems (Barabási and Albert, 1999; Brandes et al., 2013; Keeling and Eames, 2005; Latty et al., 2011). The conversion of physical networks like road systems into graphical formats has allowed analysis of their unique properties, such as the interaction of topological length (the number of road links between an origin and destination) and physical length (the same path weighted by geographic distance). This has enabled generalizable conclusions about how trips are made on a transportation network (Montis et al., 2007; Chowell et al., 2003), and varying explanations of the phenomenon of small local failures in a network leading to major system breakdowns (Kaluza et al., 2010; Barthélemy, 2014; Kalapala et al., 2006; Brockmann, Hufnagel, and Geisel, 2006; Gonzalez, Hidalgo, and Barabasi, 2008).

1.3 Accessibility

Accessibility, the ease of reaching and interacting with destinations, can be considered as the overlap between the transportation network and land use. It is a unifying concept for the planning of both, despite definitions that vary widely with the specificity of its use (Bertolini, Le Clercq, and Kapoen, 2005). The use of network analysis to analyze accessibility has risen with the development of GIS tool extensions (Liu and Zhu, 2004) and the formation of open data sources like OpenStreetMap (OSM) which allow creation of realistic network models for the analysis of sustainable accessibility (Gil, 2015). While studies have been undertaken to analyze the equity of access to facilities (Comber, Brunsdon, and Green, 2008) and impacts of improvements of transportation systems (Cheng et al., 2013), they have not focused on the effects of climate events and the joint impact on facility demand.

1.4 Facility Demand

Facility Demand Analysis has a robust body of work (Farahani and Hekmatfar, 2009), but methods typically focus around optimizing facility placement on a road network to improve service level for a single facility type (Aslam, Amjad, and Zou, 2012). Potential applications are vast, from minimizing travel times to medical facilities by locating a health center in a rural area to maximizing production for retail companies (Labbé, Peeters, and Thisse, 1995; Klose and Drexl, 2005). Various techniques have been created which seek to evaluate street networks for locating facilities, revealing that locations are strongly affected by road network structures (Zhang et al., 2016). Facility location has also been a subject of research regarding how they might affect transportation investment plans by promoting specific network links to higher hierarchical levels in the road network (Bigotte et al., 2010), especially since changing network topology is often more cost-effective than adding facilities to improve service levels (Melkote and Daskin, 2001). As with accessibility analysis, facility demand has not been widely studied in relation to the spatial extent of climate events and vulnerability. The study of disruptive incidents has primarily focused on probabilistic analysis of possible location failures (Cui, Ouyang, and Shen, 2010; Dogan, 2012) and optimizing the location of emergency response facilities in the pre-disaster stage (Salman and Yücel, 2015; Marcelin et al., 2016).

1.5 Network Vulnerability

Considered separately from facility accessibility and demand, the vulnerability of road networks to a variety of sources of degraded performance has been studied, from recurrent events like typical fluctuations in traffic to non-recurrent events like natural disasters and adverse weather (Taylor and D'este, 2003). Network science provides a convenient framework to study the vulnerability of infrastructures (Altshuler et al., 2015). Several network characteristics have been created which seek to describe the ability of a system to remain connected during a disruptive event and its aftermath. These have focused on reliability - the probability that a link, connection, or trip may maintain function in a given disruptive event. However if a link with high reliability is somehow disabled, even if extremely improbable, the consequence may be disastrous, making it necessary to value vulnerability (considering likelihood together with consequence) as a concept instead (Taylor and D'este, 2003). Scenario-based models have examined the effects of highly consequential events, regardless of their probability, by eliminating central links and recalculating network characteristics (Chen et al., 2007). Such studies seek to identify the most critical locations in a network by finding those which would have the most severe socio-economic impacts as a consequence of network failure (Taylor, Sekhar, and D'Este, 2006).

In relation to riverine flooding, one methodology to identify likely scenarios is the prediction of flood extents using the US Army Corps of Engineers' free software: Hydrologic Engineering Center's Hydrologic Modeling System (HEC-HMS) and River Analysis System (HEC-RAS) (Merwade, 2012a; Merwade, 2012b; Ackerman, 2009). HEC-HMS software allows simulation of watershed system's hydrologic processes using minimal geographic data, while HEC-RAS simulates flow through river network systems to create a number of graphical representations of riverine phenomena, including inundation extent mapping. This type of hydraulic simulation model is commonly utilized to identify and map hydrography in areas where minimal data is available, and has been applied in a broad range of international examples (Khalfallah and Saidi, 2018; Kute et al., 2014; İcaga, Tas, and Kilit, 2016; Serede, Mutua, and Raude, 2014).

1.6 Interactions in Freetown, Sierra Leone

In this analysis, we use a case study of Freetown, Sierra Leone to unify the fields of road network analysis, hydrometeorological flood extent modeling, and accessibility to facilities. To study this interaction, neighborhoods, health facilities, and education facilities are first situated on the street network. Accessibility per neighborhood to each facility is calculated based on distance to the nearest facility. Demand per facility is calculated based on the closest facility to each neighborhood and the neighborhood's population.

We then study trip generation and attraction through the analysis of Call Detail Records (CDR) provided by Africell, a mobile market leader in Sierra Leone. By applying origin-destination data to the spatial coordinates of cell towers, and calculating shortest paths between them, demand weights are applied to the road network. This is used to evaluate overall connectivity throughout the network system. Net trip generation and attraction is also calculated and applied to spatial analysis zones.

Our key contribution is twofold. First, we propose a new concept, Service Centrality (SC), which seeks to quantify the importance of individual road segments for populations to access their nearest facilities, creating a facility-based metric for use in network analysis. SC is considered jointly with demand weights to identify important road infrastructure.

Second, we assess the impact of climate events on neighborhood accessibility, facility demand, and service centrality to identify at-risk road edges. After eliminating them from the network, we reassess accessibility, demand, and service centrality. To expand upon this, we additionally consider the interaction of General Transit Feed Specification (GTFS) data provided by the World Bank, which details various public transportation information, and poverty indices calculated from Census data to better consider system changes through an equity lens.

By measuring variations in these interconnected systems, we quantify complex changes in order to facilitate the process of identifying infrastructure projects with higher co-benefits.

Chapter 2

Data

For our Freetown case study, data were taken from open sources whenever possible. However, some data were only available via the World Bank, their previous works, and access to data on officially registered facilities and detailed census data through the government of Sierra Leone. The availability of data also had a geographic component, with the majority of previous research focused around the northern section of the Freetown Peninsula where the central business district is located. This often led to the necessity of combining different data sources and methods for the northern and southern portions of the Peninsula.

Creating a generalizable method usable in low-data environments also necessitates the use of techniques that do not require a variety of proprietary software which may or may not be available to local practitioners. Therefore, whenever possible, these data were processed with free software or open source programming languages, the principal exception being the use of ArcMap for a variety of geo-spatial processing.

2.1 Population

Spatial distribution of the population is critical to socioeconomic applications, but relevant data at high resolutions is often scarce in developing nations (Gao, Zhang, and Zhou, 2019). Population data was available through the 2015 Sierra Leone Census (Statistics Sierra Leone, 2016) in two formats, which allowed for different types of analysis.

2.1.1 Population Raster

The first format utilized data available from a previous work (World Bank, 2018), which statistically distributed population data (with no additional demographic information) to a 30-meter grid based on residential building density, average number of households per residential building, and average number of residents per household, with distinctions for formal and informal housing. In that previous work, buildings data was taken from OpenStreetMap (OSM), and updated for the study through the creation of an OSM 'HOT task,' which verified and supplemented an existing database of building footprints. This was complemented in the rural areas in the South and East of the Peninsula with open source data taken from the WorldPop project (WorldPop, 2013). These 2014 estimates distribute population to a 0.0083-decimal degree (approximately 90-meter) grid based on land cover.

The World Bank's population data was aggregated to the WorldPop grid, and a mosaic raster of both grids was created for further analysis. This resulting raster shows a population distribution totaling 1,444,592 over 34,934 cells approximately 90 meters in size, with the dominant population concentration occurring on the northern coast, the central business district (CBD) of Freetown

(Figure 2.1a). Cell populations were roughly exponentially distributed, however low population cells are highly represented due to the coarser distribution of WorldPop data (Figure 2.1b).

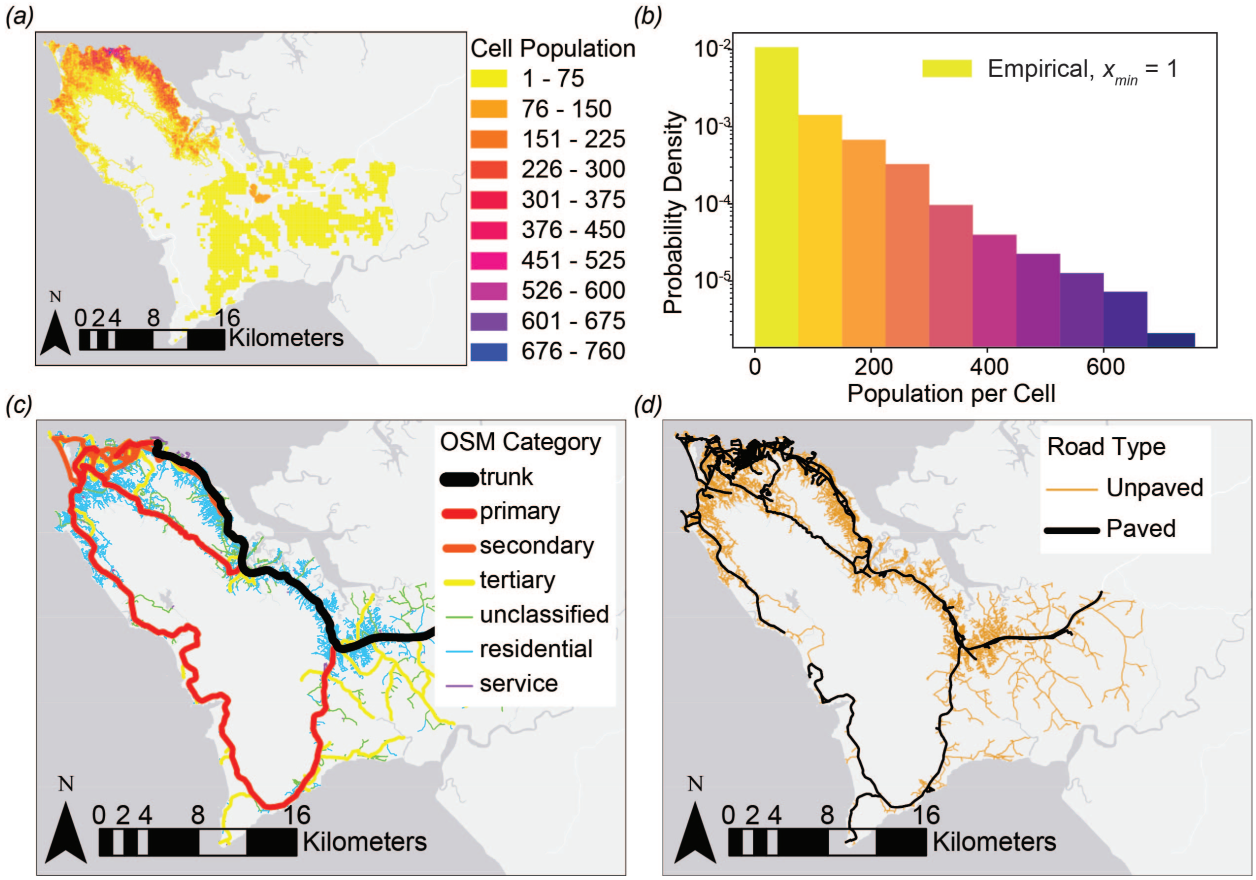

FIGURE 2.1: Input data, including: a) 1 arcsecond resolution population raster mosaic, sources: World Bank (Western Area Urban), WorldPop Project (Western Area Rural); b) Cell Population Distribution; c) OpenStreetMap road categorizations; d) paved/unpaved roads, sources: OSM, Google Earth

2.1.2 Demography by Enumeration Area

The second format contained demographic data at the level of Enumeration Area (EA), an administrative geographic unit roughly equivalent to the idea of a census tract. The Freetown Peninsula contains approximately 3,000 EAs, with 2,142 households in the rural area (Western Area Rural) and 332,006 households in the urban area (Western Area Urban) (see supplementary material, Figure A.1 for map and size distribution).

This data had coarser resolution than the population raster, but contained more richness in demographic information, including various aggregated data under the categories of Population Characteristics, Housing Status, Owned Assets, and Agricultural Practices. While the uneven distribution of population within each EA did not lend itself to our Accessibility and Demand analysis methods, we were able to use a combination of these characteristics to generate poverty indices (see Methods, below). We then used these measures to incorporate equity considerations into our analysis.

2.2 Road Network

The surface transportation network was constructed from open source data provided by OSM (OpenStreetMap, 2015), which included spatial data and information on road hierarchy and network connectivity (Figure 2.1c).

Surface type for roads was determined by the World Bank in a previous work (World Bank, 2018), however this was not extensive to the current study area. Status of Paved/Unpaved was therefore determined by visual comparison of OSM and World Bank data to satellite imagery accessed through Google Earth (Figure 2.1d).

Sierra Leone's road transport system consists of an estimated 11,555 km of roads, of which 8,555 km are classified as primary, secondary, or feeder roads, and 3,000 km are classified as local and township roads. About 1,325 km of these roads are paved, representing 11.5% of the total roads and 34% of primary and secondary roads. While 72% of the primary road network is reported in good or fair condition, only 20% of feeder roads are considered in good to fair condition. The poor state of roads and lack of transport services is considered an impediment to personal travel and goods movement. At the same time, 90% of all goods and passengers are transported via Sierra Leone's road network (World Bank Group, 2018).

2.3 Facility Locations

In pursuit of utilizing as much open source data as possible, the study originally attempted to use data scraped from Google Places to identify facilities for demand and accessibility study. Perhaps unsurprisingly, when we compared with geo-located health and education facility data from official government sources, the scraped data was found to be highly inadequate in comparison and not representative of either the number or distribution of facilities across the Freetown Peninsula. Therefore, for this study, the government logs of registered health and education facilities were used to calculate these metrics.

Health locations are divided into three main categories: hospitals (n = 44), health centers (n = 164), and pharmacies (n = 50). Education facilities are divided into four main categories: senior secondary schools (n = 208), junior secondary schools (n =353), primary schools (n = 746), and pre-primary schools (n = 532). In all categories, education facilities outnumbered health facilities, resulting in access and demand variations that facilitated different approaches to analysis.

2.4 Call Detail Records

Anonymized CDRs were provided by the Africell mobile phone service provider from 7AM – 10AM during the months of January, February, June, and July. These record connection of mobile devices to indexed cell phone towers. When mobile activity is recorded at a cell phone tower, this indicates that a user is within the same geographic area. Tracking the same user's activity from tower to tower over the course of a day gives an idea of their travel activities. With a large dataset, this can be aggregated to create a general idea of trip generation for a population in a region.

We used parameters to define active users as indicated in Table 2.1. Filtering users by these parameters created a refined dataset with the characteristics indicated in Table 2.2. Finally, trips were aggregated and assigned to an origin-destination (OD) matrix based on the index of cell phone towers for origins and destinations. Trips were defined according to the parameters indicated in Table 2.3.

TABLE 2.1: Parameters for selecting active users

Parameter	Definition
Threshold for average number of calls per day	3 times overall average
User identification	Phone number
Threshold for proportion of days with events	0.6
Required number of users	6,000,000

TABLE 2.2: CDR dataset metadata

Characteristic	Value
Median average calls per day	0.25
Mean average calls per day	2.8
Median proportion of days with calls	0.09
Mean proportion of days with calls	0.27
Number of users before filtering	6,624,881
Number of active users (after filtering)	650,961

TABLE 2.3: Parameters for trip generation

Characteristic	Value
Minimum stay time for a location	30 minutes
Distance threshold for a trip	2 km
Required trip hours	07:00 - 10:00

Within the study area, a total of 2,505,428 trips were generated over the three-hour period during the course of four months, or an overall average of 6,960 trips per hour.

Aggregating trips for morning hours creates a picture of AM peak travel activity. Areas with a high influx of trips indicate geographies with a high number of attractive points of interest, such as places of employment, which may signify a Central Business District (CBD) in an urban geography. Areas with a high outflux may indicate primarily residential areas which generate trips into attractive areas.

Indexed cell phone tower locations were also provided with latitude and longitude coordinates. These allowed analysis zones to be generated which, when considered with origin-destination pairs, create trip generation and attraction patterns grounded in the geography of the combined Freetown Western Area Urban and Western Area Rural.

2.5 General Transit Feed Specification

The World Bank has provided transit specifications in GTFS format. This data includes information on unique routes, headway, fare, and spatial extent.

Since the primary focus of this study is the spatial interaction of Freetown's road network with environmental factors, this study focuses on spatial extent of unique routes (see supplementary

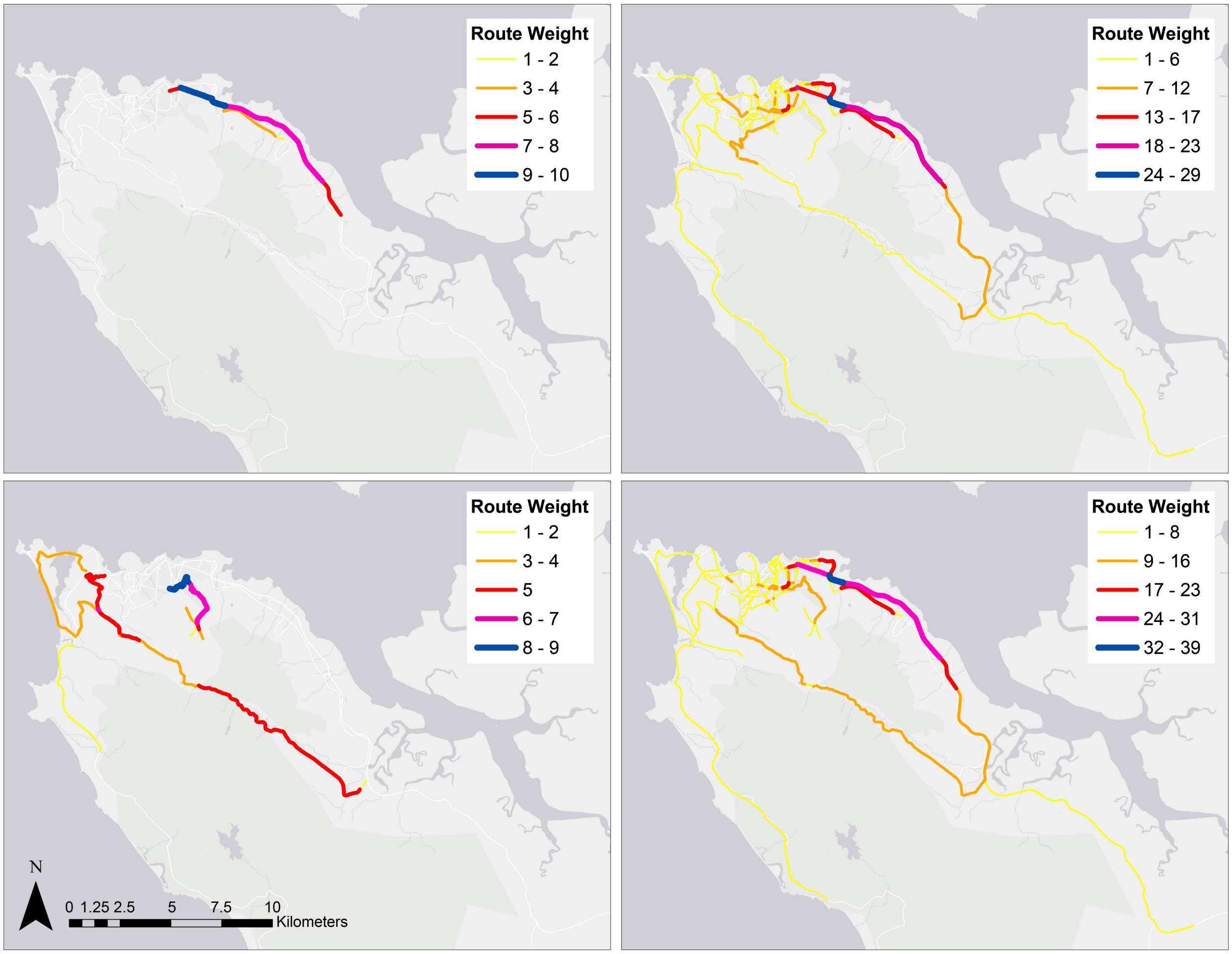

FIGURE 2.2: Road network, weighted by number of unique transit routes for commercial bus (upper left), poda poda (upper right), taxi (lower left), and combined (lower right)

material, Figure A.2 for details). However, visualizations of average headway and fare by route and mode are also provided in Supplemental Figures A.3 and A.4, respectively. We can generally categorize these modes by saying that in order from commercial bus to poda poda to taxi, these modes have smaller headways and greater fares.

Additionally, it is evident that poda poda is the most diversely utilized mode, with the greatest spatial extent and most variety of routes. Among the modes, poda poda also represents the middle in both costs and headways.

2.6 Environment

Following the Regent-Lumley Disaster in Freetown, we considered riverine hazards as our primary interest. Previous work assessed riverine risk generally, primarily using spatial buffers around known river centerlines to assess general proximity of road infrastructure to flooding hazards (Nelson et al., 2019). This study seeks to expand on the accuracy of floodplain estimations through the use of well-documented methodology using the US Army Corps of Engineers' free software: HEC-HMS, HEC-RAS, and their related plug-ins for use with ArcMap (Merwade, 2012a; Merwade, 2012b; Ackerman, 2009). This procedure, described in detail in Methods below, requires several data sources:

2.6.1 Land cover

Detailed land use data was not available for Freetown, so basic geographic data provided by the World Bank was verified against satellite imagery accessed through Google Earth. Shapefiles were developed using ArcMap to classify land cover into four basic categories - water, medium residential, forest, and agricultural - according to the USGS Land Cover Classification System (Anderson, 1976).

2.6.2 Soil type

Detailed soil data was not available, so we utilized Zobler's 27 Great Group level type classification system and map (1999), which provides soil classification at a 1-degree resolution (Zobler, 1999).

2.6.3 Curve number

Runoff Curve Numbers are parameters which help predict runoff and soil infiltration. This number is calculated using Land Use and Soil Types indicated above via a Curve Number Look-Up Table (Cronshey, 1986).

2.6.4 Elevation

Ultra-high resolution digital elevation models (DEM), such as those created using LIDAR methods, were not available. The highest resolution elevation data was available through ASTER Global DEM, a product of METI and NASA. Resolution is 1 arcsecond, equivalent to approximately 30 meters (NASA/METI/AIST/Japan Spacesystems, 2009).

2.6.5 Satellite imagery

Since the ASTER Global DEM is known to have various inaccuracies and artifacts, it is crucial to check evident river and drainage centerlines against satellite photographs to identify necessary corrections. Google Earth was used as a source in this regard to manually correct artifacts in the DEM.

2.6.6 Hydrometeorology

Meteorological and river flow data is extremely limited in Sierra Leone. The World Bank previously contracted with a consultant to estimate 20, 50, 100, 200, 500, and 1,500 year flood events using rainfall-runoff models simulated with proprietary software for the Northern Peninsula only. We used empirical precipitation data from the 2017 Regent-Lumley mudslide, which was conditioned and triggered by a 200mm accumulated rain event over approximately 7 days. This corresponded to at least a 100-year flood extent according to the World Bank's previous estimation (World Bank, 2018).

Additionally, local seasonal road flooding hazard data, detailing geography, extent and severity, was collected by engineering students at a local university in partnership with the World Bank. By comparing this data to recorded major flood extents and estimates, we determined that minor flooding caused by non-catastrophic events does not correlate geographically with riverine flood extents. This inspired additional analysis undertaken in the Results section, "Effects of seasonal flooding hazards," below.

Chapter 3

Methods

The primary consideration for this study was the effect of climate events on system connectivity as well as access and demand for facilities. However, to analyze these effects, a base scenario was first determined as a point of comparison.

3.1 Estimation of Population Centers

To reduce the calculation time for our multi-phase analysis and gain insights into how populations were distributed, the study first reduced the number of population cells from approximately 35,000 cells of identical size and highly variable population to a smaller number of aggregated neighborhoods with varied sizes and approximately equal populations. An aggregation algorithm was created, primarily using Python's shapely package. This merged population polygons, in order from largest to smallest, with adjacent neighbors conditional upon whether the merge would fall within a set lower and upper limit. The largest population size of a single cell was 756, so to approximate this size for created neighborhoods, the lower limit was set to 700 and the upper limit was 900. This resulted in 2088 neighborhoods with median population of 771, with 83% of neighborhoods falling between populations of 600 and 900 (Figure 3.1a, see supplementary material, Figure A.5 for details).

Since this method uses only physical adjacency (shared borders) to determine whether population cells should be merged, it is generalizable to units of any shape or size.

3.2 Accessibility

For this study, accessibility to a given facility is defined as the distance along the road network's shortest path from a given neighborhood to the nearest facility by road. To calculate this, centroids of the newly created neighborhoods were determined. Then, the Pandana package in Python was used to calculate distances from each neighborhood centroid to its nearest facility based on its distance-weighted shortest path (Figure 3.1b). Calculated distances approximated lognormal distributions (Figure 3.1c, see supplementary material, Figure A.6 for health facility distribution).

Among the seven facility types, it could be expected that the maximum distance from a neighborhood would increase as the number of facilities decreased. However, there are significant exceptions to this in the case of Freetown. The highest maximum distance is to pharmacies, where the worst off neighborhood must travel 46km to reach the nearest facility. In comparison, hospitals have six fewer facilities, but the maximum distance to reach them is 26km. This reflects a tighter concentration of pharmacies in Freetown's CBD, whereas hospitals are more evenly distributed. We can expect that this will present greater challenges to maintaining access during climate events, particularly for rural populations.

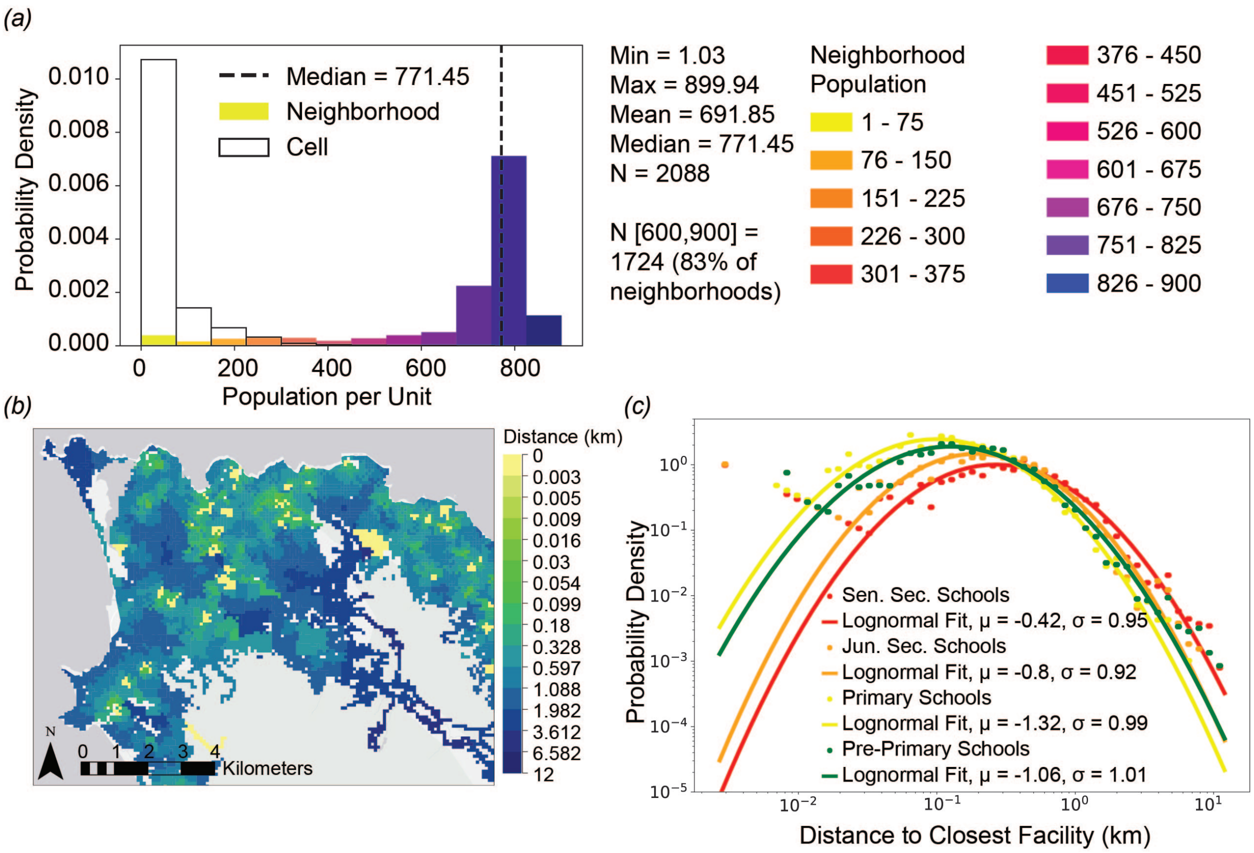

FIGURE 3.1: Neighborhood Generation and Accessibility Calculation: a) Neighborhood population distribution compared to cell population distribution with key information; b) Neighborhood distance to Senior Secondary Schools; c) Distribution of neighborhood distance to education facilities

3.3 Facility Demand

Neighborhoods were also assigned identification numbers for their nearest facilities, allowing demand for each facility to be assessed. ArcMap was used to aggregate neighborhoods by their assigned facilities to determine service areas and aggregated population totals (see supplementary material, Figures A.7, A.8, A.9, A.10, A.11, A.12, A.13 for details).

The resulting distributions reinforce what accessibility analysis suggests by reflecting widely varying demands depending upon facility type. The top quartile of facilities ranges from serving 51.1% of the population for Primary Schools to 87% of the population for Pharmacies. The top three facility types with the worst upper quartile are Pharmacies, Senior Secondary Schools (62.4%), and Health Centers (62.3%), reflecting the uneven distribution of their locations in the Freetown CBD. See supplementary material, Figure A.14 for more information on the interaction between service area and population served for all facility types.

3.4 Poverty Analysis

Using the demographic data by EA, we carried out detailed poverty mapping, accounting for a variety of factors that are indicative of poverty using methods undertaken by the World Bank in a previous work in Ghana (IBRD/The World Bank, 2015). This method uses available census data regarding housing and non-housing factors to create a poverty "score" for each EA.

The housing factors considered to contribute to poverty include the type of dwelling, main construction materials, tenancy, sanitation, and main sources of lighting, water, and cooking fuel. Scores range from 1 for choices indicating low chance of poverty to 5 for choices indicating high chance of poverty, with some "Other" choices receiving a score of 0. Considering the available choices for each of the eleven indicators, this translates to a minimum score of 2 and a maximum score of 55. The specific criteria for different scores are listed in Table 3.1 below:

TABLE 3.1: Detailed poverty mapping indicators (housing variables)

Housing Variables	0	1	2	3	4	5
Type of dwelling unit		Separate house; Semi-detached house	Flat/Apartment	Compound house (rooms); Other	Huts/Buildings (same compound); Huts/ Buildings (different compound)	Tent; Improvised home (kiosk, container, board, pan-body); Uncompleted building
Major material for construction of wall	Other	Stone; Cement Blocks	Clay Bricks; Burned Bricks	Sandcrete; Mud Bricks; Mud & Wattle	Zinc; Timber	Poles/Reed; Tarpaulin
Major material for construction of floor	Other	Stone	Tiles	Wood	Cement	Mud
Major material for construction of roof	Other	Tiles	Concrete; Asbestos	Zinc	Thatch	Tarpaulin
How was dwelling acquired?	Other	Owner-Purchased; Owner-Constructed; Owner-Inherited	Renting Government; Renting Housing Corporation; Renting Private; Renting-Parastatal/Quasi-Government	Employer-Government; Employer-Parastatal/Quasi-Government	Employer-Private	Squatter
Principal source of lighting	Other	NPA/BKPS	Generator; Solar	Gas; Kerosene	Battery/ Rechargeable Lite; Candle	Wood
Principal source of drinking water	Other	Piped indoors	Piped in compound; Mechanical Well	Protected Ordinary Well; Protected Spring; Sachet/Bottled Water; Water Vendor/Bowser	Public Tap; Unprotected Spring; Neighbour's Tap	Unprotected Ordinary Well; River/Riverbed/ Stream
Principal source of water for household use	Other	Piped indoors	Piped in compound; Mechanical Well	Protected Ordinary Well; Protected Spring; Sachet/Bottled Water; Water Vendor/Bowser	Public Tap; Unprotected Spring; Neighbour's Tap	Unprotected Ordinary Well; River/Riverbed/ Stream
What is your principal source of fuel supply for cooking?	Other	Electricity; Gas; Solar	Kerosene	Charcoal	Wood	Crop Residue; Saw Dust; Animal Waste
Kind of bathing facility		Inside	Outside; built	Outside; makeshift	Other	None
Type of toilet facility	Communal-Other; Private-Other	Communal-Flushed inside; Communal-Flushed outside; Private-Flushed inside; Private-Flushed outside	Communal-VIP; Private-VIP	Communal-Pit; Private-Pit	Communal-Bucket; Private-Bucket	Communal-Bush/River bed

Non-housing factors include illiteracy, school attendance, unemployment, child death rate, and adult deaths within the last 12 months. Scores of 1 to 5 are applied here based on quintile, so scores in the lowest 20% of the region would have a score of 1 through to scores in the highest

20% of the region which would have a score of 5. With six indicators, this translates to a minimum score of 6 and a maximum score of 30. The specific criteria for non-housing indicators are listed in Table 3.2 below:

TABLE 3.2: Detailed poverty mapping indicators (non-housing variables)

Non-Housing Variables
Proportion of residents who are illiterate
Proportion of residents who have never attended school
Proportion of residents who are unemployed
Child mortality rate
Proportion of households that have experienced deaths in the 12 months previous to the census
Household size

By considering housing and non-housing indicators, we can gain a comparative understanding of poverty in the region. High-scoring EAs are more likely to display high rates of poverty compared to low-scoring EAs. While, unlike poverty systems in the United States, this does not provide a percentage of the population that falls under a certain "line," it does provide a useful way to refer to areas which are more economically strained than others.

See supplementary material, Figure A.15 for a detailed map of calculated poverty indices.

3.5 Estimation of Analysis Zones

We used the CDR data to better understand how trips were conducted between different areas on the Peninsula. A Voronoi diagram was created based on the point locations of cell towers. A Voronoi diagram partitions an area into regions based on the position of point features. Within each of these regions, all points that lie within it are closest to the same point feature.

As it relates to this study, a mobile device that connects to a given cell tower might be located anywhere within the surrounding polygon. The centroid (center of mass) of a such a polygon is likely to represent the average location of all users connected to that tower. Therefore, centroids were calculated to create points that are representative of each cell tower zone for subsequent spatial calculations and network analysis.

To illustrate, Supplemental Figure A.16 shows the Freetown Peninsula partitioned in a Voronoi diagram by cell tower point features.

3.6 Road Network

3.6.1 Overall Connectivity

The overall connectivity of the road network is described using an augmented edge betweenness centrality metric (BC^{aug}). This method uses trip data from an OD matrix to estimate demand flows on a network using an augmented betweenness centrality metric (Puzis et al., 2013). This has a relatively complex reasoning which is best described in a progression.

Shortest path betweenness centrality denotes the total proportion of shortest paths between every pair of nodes in a network which pass through a given node of interest. This can also be expressed as edge betweenness centrality (BC) which quantifies the shortest paths passing through a link, rather than a node.

Shortest paths can be defined in a number of ways. In a non-physical network, shortest path is defined by the path taking the fewest links between any two nodes (also known as hop-counting), which is not a good method for a reasonable traffic assignment model. Instead, BC can be augmented by calculating Dijkstra shortest paths. These use a link weight to calculate shortest path. In our study, we use the physical length of a link to calculate shortest path. Since we lack information on speed limits or traffic flow patterns, this can be considered as proportionate to the free-flow travel time which is used in the Puzis study.

However, BC still assumes equal weights between every pair of nodes in the network. We augment BC further by weighting shortest paths by the number of trips in a measured OD matrix, while continuing to assume that routes will follow the distance-weighted shortest path. In this case, special nodes representing cell tower zones are identified by their proximity to the centroids of the cell tower polygons created in the Voronoi diagram. Origins and destinations in the matrix therefore correspond to specific nodes in the network where trips are produced and received in concept.

Demand weight is therefore calculated by:

$$Demand(v) = \frac{\sum_{i \neq v \neq j} \frac{\sigma_{ij}(v)}{\sigma_{ij}} \cdot OD_{ij}}{\sum_{i \neq j} OD_{ij}} \tag{3.1}$$

Where v is any edge, σ_{ij} is the distance-weighted Dijkstra's shortest path between unordered node pairs i and j, $\sigma_{ij}(v)$ is the number of those shortest paths which pass through v, and OD is the trips measured in an origin-destination matrix.

Demand weight is therefore the percentage of total trips that pass through a given link on their distance-weighted Dijkstra's shortest path. This is visualized in Figure 3.2.

Puzis et al. found that this augmented betweenness centrality metric correlated well with measured traffic flows. However, they noted that a few high-congestion links exhibited high values compared to real traffic flow. This aligns with the idea that traffic assignment is unlikely to follow free-flow travel time in congested corridors. We are, however, prohibited from making further refinements recommended in their study by a lack of road capacity or traffic flow information in Freetown. Future study would benefit from collection of such data.

3.6.2 Facility Connectivity

For connectivity to facilities, we propose the concept of Service Centrality (SC). We define SC as the percentage of a study area's population that passes through a link to access its closest facility via the distance-weighted shortest path.

SC is therefore calculated by:

$$SC(v) = \frac{\sum_{kl} \frac{\sigma_{kl}(v)}{\sigma_{kl}} \cdot NF_{kl}}{\sum_{kl} NF_{kl}} \tag{3.2}$$

Where v is any edge, σ_{kl} is the distance-weighted Dijkstra's shortest path between the road network node closest to the centroid of neighborhood k and the road network node closest to the facility l nearest to k, $\sigma_{kl}(v)$ is the number of those shortest paths which pass through v, and NF is a matrix assigning population values for neighborhood k to closest facility l.

SC can be calculated for a specific type of facility, or it can be an aggregate of multiple facility types, based on need. For this study, we calculate SC both for individual facility types and for aggregate facility types like Health, Education, and Overall. We then use these different SC metrics for various applications of accessibility and demand analysis.

To calculate SC, we used OSMnx, NetworkX and Pandana packages in Python to determine shortest paths between neighborhoods and their nearest facilities, assigning neighborhood population to them as a weight. We then aggregated demands for all neighborhood-facility combinations to the road network links and divided them by total population to calculate percentage. SC was calculated for all individual facility types, health facility aggregate, education facility aggregate, and overall aggregate. Figure 3.3 provides a visualization of this concept while supplemental Figure A.17 describes the interaction of Demand and SC.

3.7 Trip Production and Attraction

Since the method described in Road Network Demand above uses Voronoi diagram centroids to identify origin and destination nodes on the road network, productive and attractive nodes can be identified using the concepts of Weighted Indegree and Weighted Outdegree.

The general weighted degree of a given node represents the total weight assigned to links connected to it. In a directed network where the direction of a connection matters, this is further specified. Indegree totals the weight of links directed into a node, while outdegree totals the weight of links directed out of the node. For the purpose of our study, the weight here is considered as the non-normalized numerator of Equation 3.1. It therefore represents the aggregate AM trips over the entire four-month period.

Every node in a directed network will have an indegree and an outdegree. By calculating the difference between these, we can identify the network nodes from which net trips are coming or going. Based on the methodology detailed in the previous section, this is always the network node identified with the cell tower Voronoi diagram centroids.

Supplemental Figures A.18 and A.19 visualize this concept. Blue and red dots respectively indicate the net attraction (indegree - outdegree) or net production (outdegree - indegree) calculated based on the network demand weights.

3.8 Hazard Estimates

To identify parts of the system that were vulnerable to flooding, we first sought to identify the parts of the road network that intersect with likely flood extents. As previously mentioned, we focused both on major hazards caused by severe riverine flooding and seasonal hazards caused by expected levels of seasonal precipitation.

3.8.1 Major Flooding Hazard:

The combination of remote sensing and GIS techniques has become popular in flood estimation methods (Gao, Zhang, and Zhou, 2019). As previously mentioned, one such flood extent modeling method using HEC-HMS and HEC-RAS is summarized in Figure 3.4. For this study, relatively coarse elevation data in combination with other data indicated above were reconditioned to correct obvious artifacts and coincide with drainage patterns of known rivers and drainage lines (confirmed through satellite imagery). Characteristics of each river basin, such as flow direction and accumulation were calculated using the HEC-GeoHMS extension in ArcMap. These river basin hydrological models were exported for processing in HEC-HMS, where the above-mentioned meteorological data was used to generate a steady rate of precipitation as an input to flood models.

Nineteen drainage channels were modeled using the HEC-GeoRAS extension in ArcMap, using results from HEC-HMS as inputs to determine flood extents. The results of these inputs were validated against known floodplains, particularly those which resulted from the 2017 Regent-Lumley Mudslide, as well as flood extents generated in the World Bank's previous work. Model results closely mirrored both the extent of the 2017 event and the 100-year floodplain, so we proceeded with these inputs for floodplains in previously unstudied areas. Where possible in the Northern Peninsula, previously generated 100-year flood extents were prioritized over newly generated flood extents due to the increased sophistication of the former method. The resulting flood extent map, shown in supplemental Figure A.20, is a mosaic of the two methods.

3.8.2 Seasonal Flooding Hazard:

It is important to consider the effects of seasonal precipitation conditions on roads as well. Since, in general, locations of minor local flooding did not correlate closely with riverine flooding, we identified areas of low slope (less than five degrees) and areas that lacked external drainage, or elevation "sinks," which would intuitively lead to the accumulation of water on irregular surfaces such as poorly maintained unpaved roads with insufficient drainage. The extents of these areas were calculated in ArcMap using the Aster DEM and merged to determine extent (see supplementary material, Figure A.21 for details), and were found to correlate with the local event data.

Unlike the Major Flooding Hazard extent map, the Seasonal Flooding Hazard extent map is not intended to realistically model extents of a single event. Instead, it is meant to identify areas in which poor road conditions are more likely to be exacerbated by seasonal urban flooding due to unsuitable stormwater drainage. These suppositions could be better informed by higher-resolution DEMs such as those created using LIDAR technology, which could easily be plugged into the method.

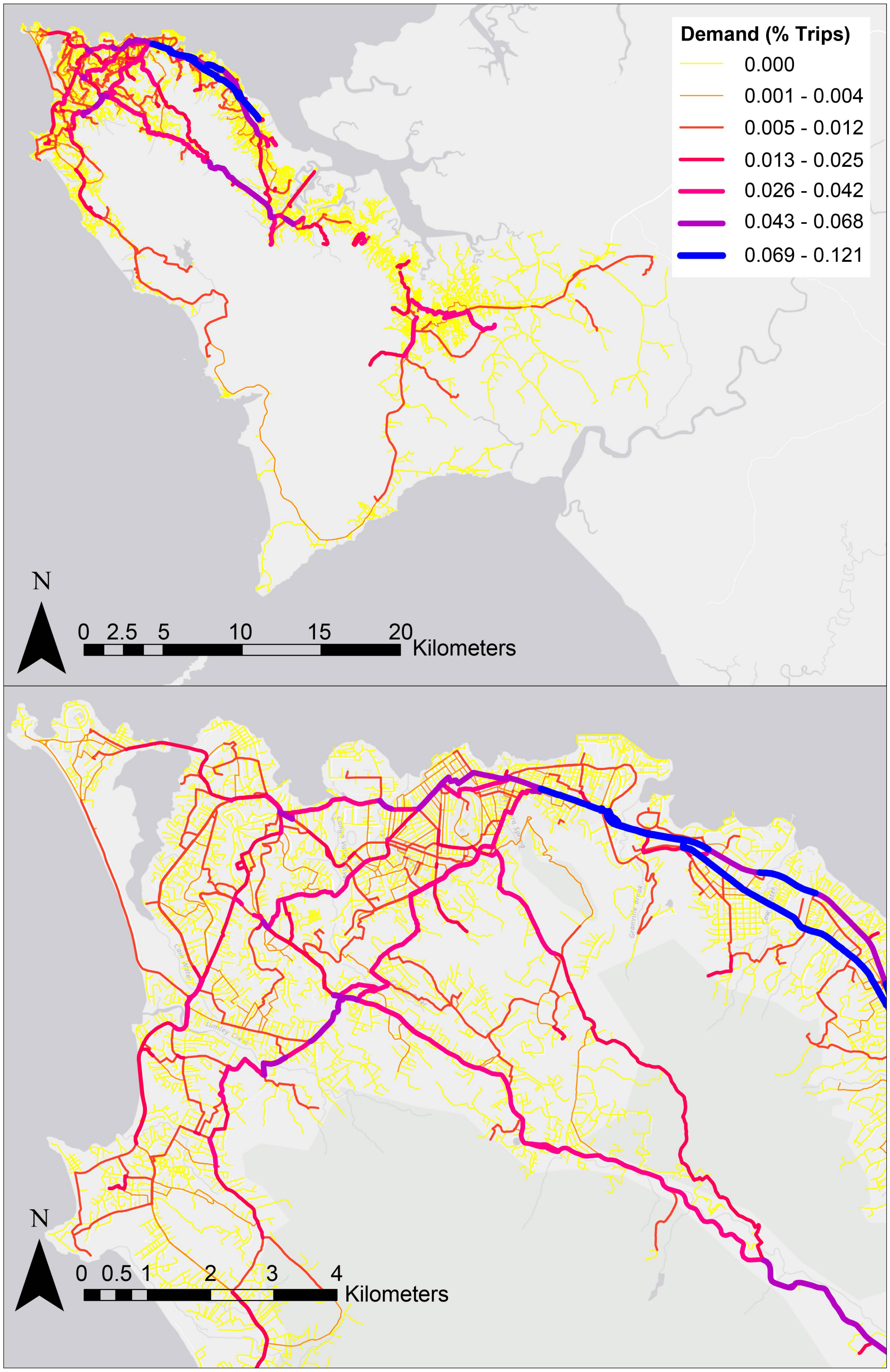

FIGURE 3.2: Distance-weighted road network links show high usage of Bai Bureh road on the Northeast coast of Freetown Peninsula, likely due to the high incidence of trips to Freetown's CBD. Within the CBD, lower-hierarchy roads diffuse demand throughout the area.

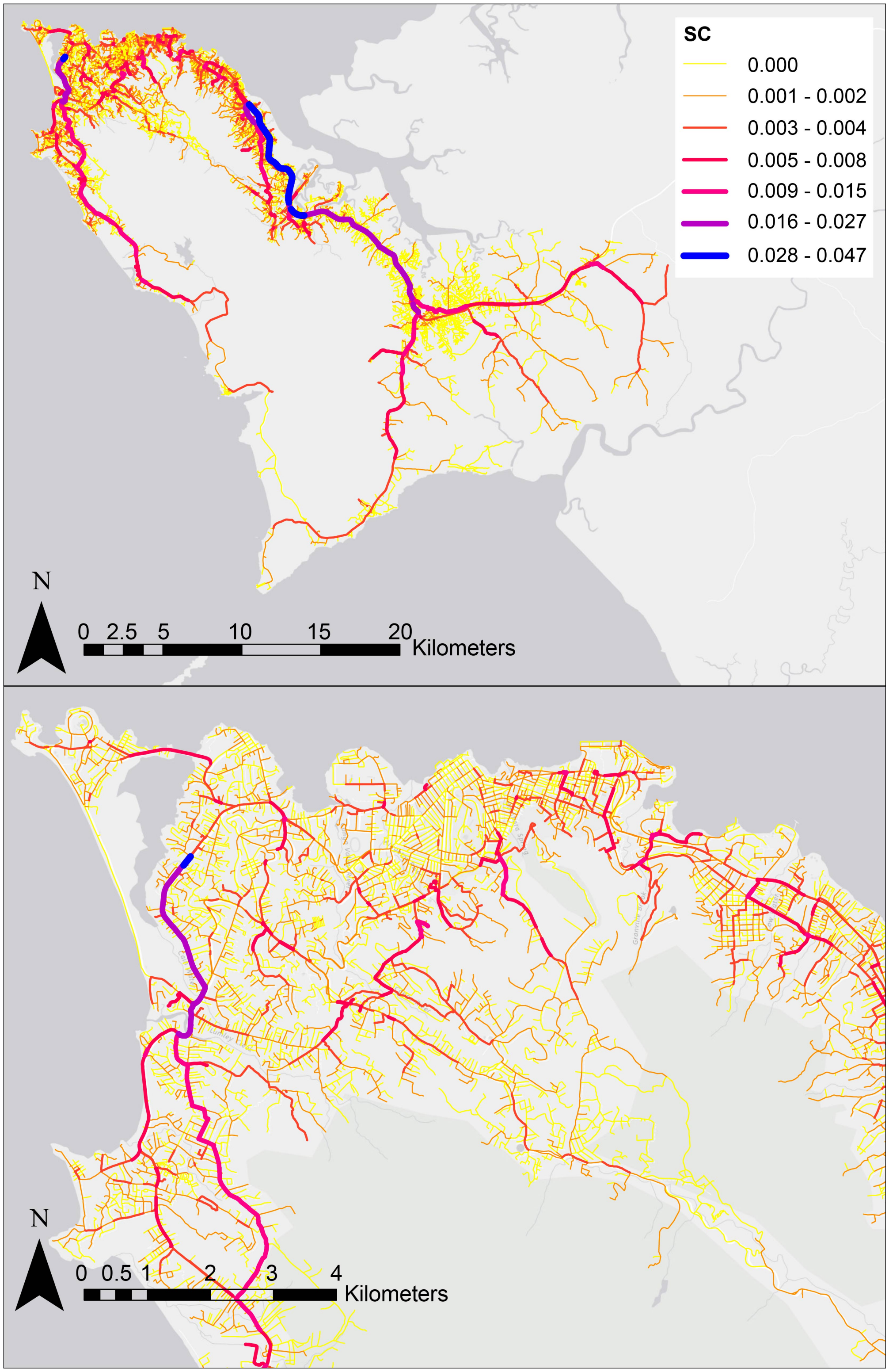

FIGURE 3.3: Service Centrality for all facilities shows a distribution throughout the network that is not strongly directional. The complex interaction of shortest paths to multiple facilities often highlights road segments as important which may not appear so otherwise

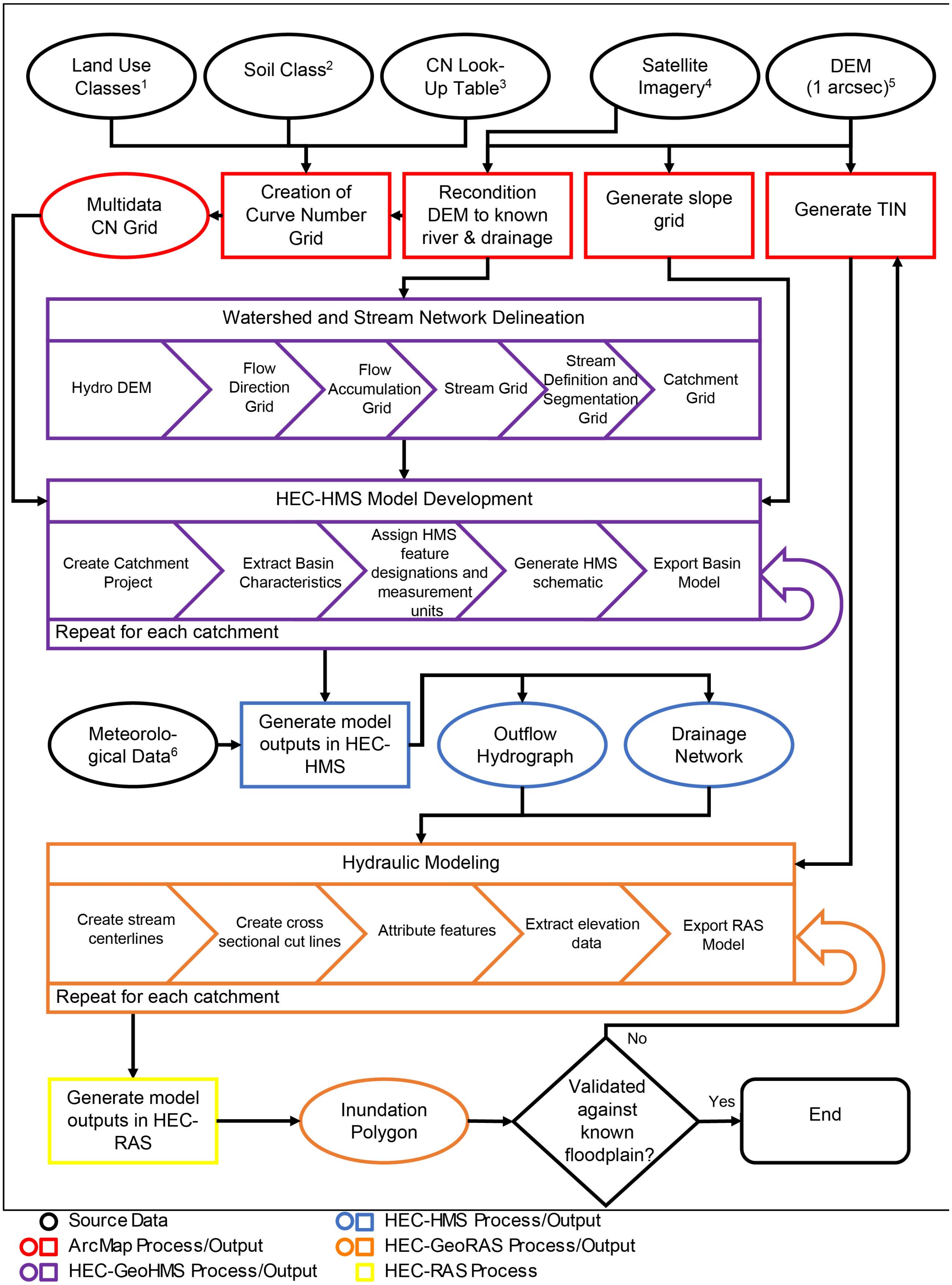

FIGURE 3.4: Method to estimate the extent of Major Flooding Hazards

Chapter 4

Results

We apply the proposed methods in two key ways: Major Flooding Hazards and Seasonal Flooding Hazards. Major Flooding Hazards are those which result from significant riverine flooding. In this case, scenarios are identified in which roads vulnerable to these specific weather events are disabled, and the key metrics of BC, SC, Service Accessibility, and Facility Demand are recalculated to examine system changes under the new conditions. Seasonal Flooding Hazards are those which result from expected levels of seasonal precipitation. Here we quantify exposure of roads to localized flooding within individual service areas to identify which neighborhoods and service areas are most vulnerable to these effects.

4.1 Effects of Major Flooding Hazards

In our initial data exploration, we observed that health services in the study area had a significantly lower availability than education services. As a result, certain roads became very important to access the nearest facilities, particularly for residents in the rural areas in the southeast. The increased importance of these roads implied that the consequences would be greater if they were completely disabled. Therefore, we determined that analyzing Health SC in combination with major flooding hazard extent would be of particular interest.

To illustrate this selection process, Figure 4.1 demonstrates how links were identified for Scenario 1. Roads with high Health SC that coincide with flood extents are more likely to be disabled, and if they are disabled, stand to more significantly disrupt access to services. In Scenario 1, two bridges are disabled which serve as the only links between the more rural southeastern Peninsula and the central business district in the north.

As an example, Figure 4.2 describes the effects that disabling these key bridges would have on accessibility and demand for hospitals. Figure 4.2a shows shifts in demand between two facilities, with 1.6% of the population of Sierra Leone shifting from their closest hospital to the next closest. This significant change might lead to difficult strains on this hospital's resources, a particular problem if needs simultaneously rise due to the occurrence of a dangerous natural disaster. Additionally, Figure 4.2b illustrates that the neighborhoods affected by this shift must travel up to 6.7 km farther to reach the nearest hospital. Again, increases in distance to nearest facility might prove dangerous or fatal in an emergency situation.

Supplementary Figures A.22 and A.23 show similar analysis for Health Center and Pharmacy facilities. While affected Health Centers experience small demand shifts and increased travel distances of less than 1km, Pharmacies experience drastic shifts resulting from their tight concentration in the central business district (CBD). The entire rural population of the Southeastern Peninsula is forced to travel up to an additional 63km along an alternate route to reach the CBD, greatly reducing access to pharmacy goods and services. Additionally, the affected population is approximately 9.6% of the total, resulting in a drastic demand change for the next nearest pharmacy.

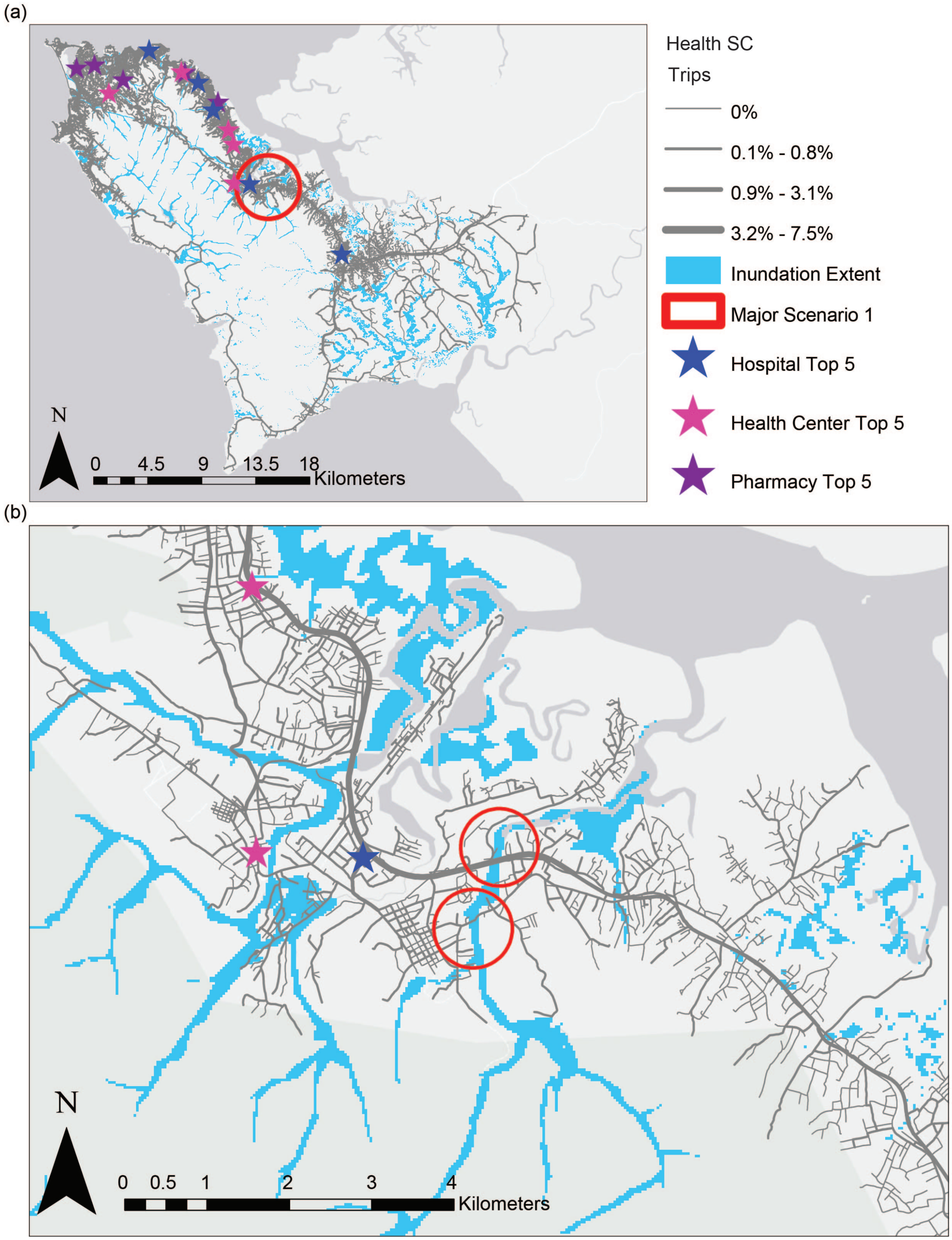

FIGURE 4.1: Coupling demand and service areas of top Health facilities areas with the estimates of major climate events: a) Scenario 1 identified on Freetown Peninsula; b) Detail of Scenario 1 indicating specific affected links

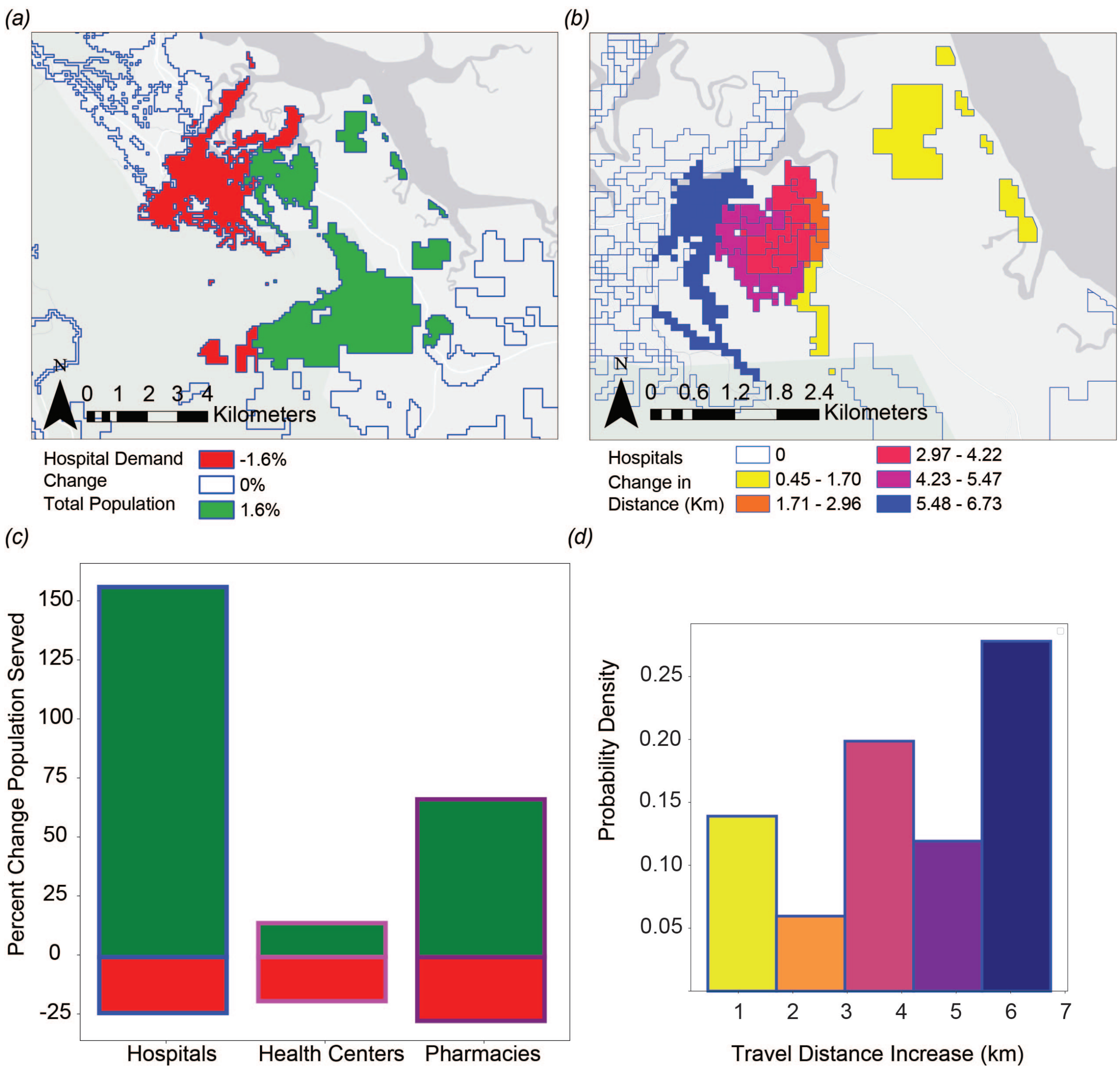

FIGURE 4.2: Disruptions of Major Flooding Hazards, Scenario 1: a) Demand shifts for affected hospitals; b) Hospital accessibility shifts for affected neighborhoods; c) Distribution of demand shifts for affected hospitals; d) Distribution of hospital accessibility shifts for affected neighborhoods

Figure 4.3 further quantifies these changes by reexamining road network characteristics in several scenarios. If important links are disabled, roads experience shifts in both SC and overall connectivity as expressed by Demand weight (see supplementary material, Figure A.24 and A.25 to see how Figure 4.3 is divided between Demand weight and SC). Roads that experience positive shifts in both characteristics represent a drastic increase in importance both to the network system and the population's access to facilities. This is clearly shown in Scenario 1 where the western coastal highway becomes a crucial artery. Scenario 2 exhibits that even a small shift in the geography of an event can have drastic effects on a system. Compared to Scenario 1, the slight

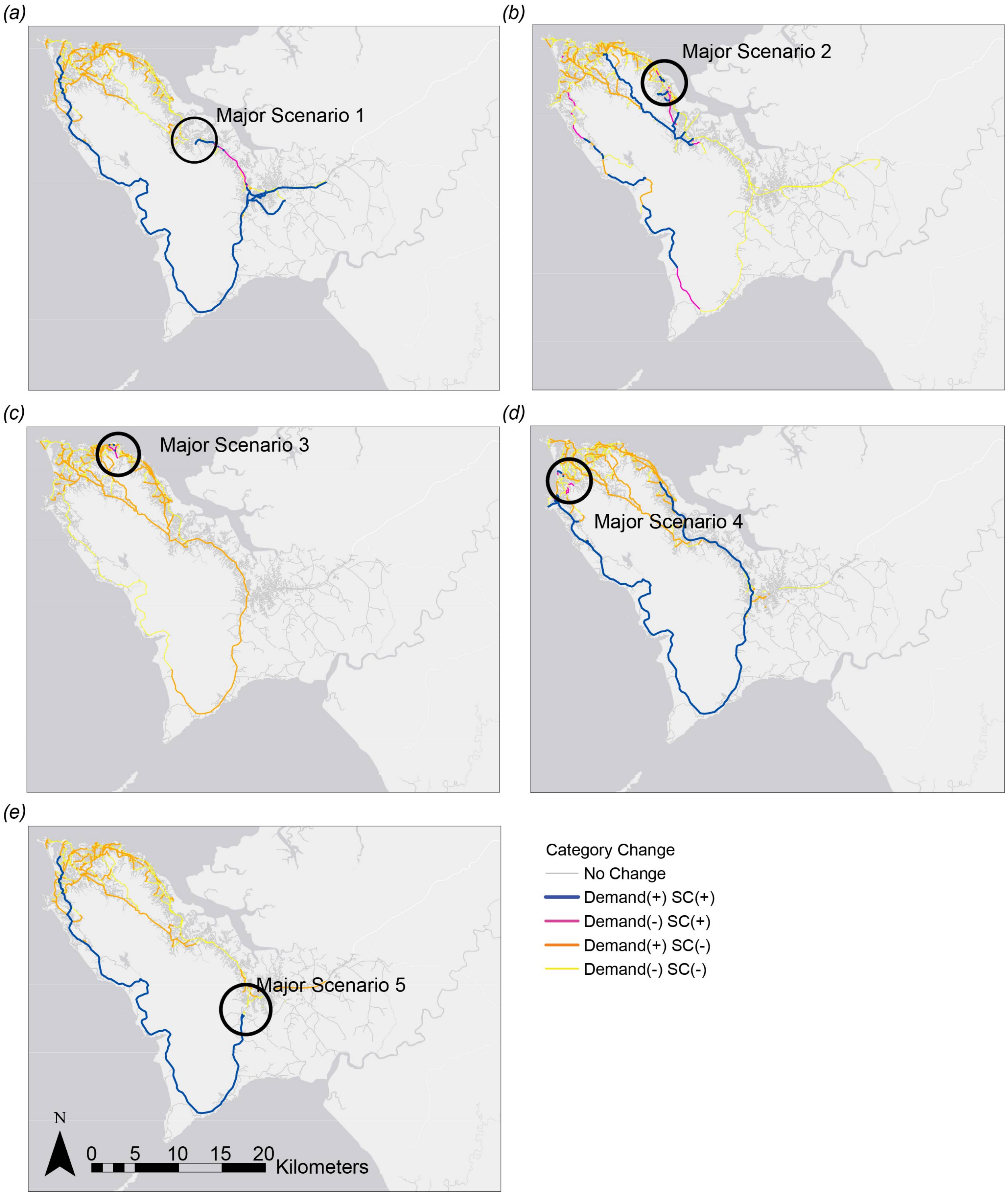

FIGURE 4.3: Changes in Road Categorization under Major Flooding Hazard scenarios, disabled roads in: a) Scenario 1 - rural area, b) Scenario 2 - north on major highway, Bai Bureh Road, c) Scenario 3 - in the Freetown central business district, d) Scenario 4 - in the 2017 Regent-Lumley Disaster area, and e) south of the rural Waterloo area

northern shift of the event has increased the importance of the central roadway rather than shifting all demand to the western coastal highway. Scenario 3 shows that events in highly connected and developed areas with higher incidence of facilities, such as the CBD, stand to have little effect on the system's SC even when overall connectivity is decreased throughout the system. Scenario 4 recreates the Regent-Lumley disaster of 2017, again showing the increased importance of the Western Coastal highway for both connectivity and access to services in disaster scenarios. Finally, Scenario 5 shows that even if infrastructure is disabled in rural areas, system impacts can have wide-ranging geographies.

Using these methods, governments and lending institutions can help compare the possible effects of improving a given connector within a road network system and quantify the benefits of improving it, or the drawbacks of neglecting it. These methods are applicable to any type of facility or combination of facility types at multiple scales.

4.1.1 Poverty Implications

The scenario-based methodology can also be used to examine how different events may impact accessibility from an equity lens. To accomplish this, we identified shifts in hospital accessibility for neighborhoods in the Freetown Peninsula and overlaid affected areas with poverty-indexed EAs.

To overcome the spatial mismatch between EAs and generated neighborhoods, we first generated critical zones by dissolving the borders between neighborhoods shown to have their accessibility negatively affected by a Major Flooding Hazard. After normalizing each poverty indicator to one, we created a combined score ranging from 0 to 2. We then found the intersection of this poverty map with the critical zones and calculated an average poverty score per critical zone by weighting the score of each EA by its area.

Figure 4.4 visualizes each critical zone with its averaged poverty score. Scenarios 1 and 5 represent populations who are significantly more exposed to poverty, while Scenario 3 affects neighborhoods that have the least poverty exposure. This is not surprising since the poverty scores visualized in Supplementary Figure A.15 tended to increase with distance from the CBD. To that end, while it may be tempting to produce projects in the city center, focusing infrastructure improvements which reduce accessibility shifts in more vulnerable neighborhoods like in the rural southeast may go farther toward reducing social risk in Freetown overall.

4.1.2 Transit Implications

The analysis and development of transit systems can also be supplemented by this analysis. In this study, we seek to identify those transit routes which are the most critical both for use during normal conditions and in the event of Major Flooding Hazard Scenarios. To accomplish this, we calculated road network areas which are important under both of these criteria. Then, we identified which public transit routes provide the most service through these areas and quantified their coincidence.

Figure 4.5 describes the method through which these areas were selected. Part a) shows the identification of important network areas under normal conditions by illuminating only those which are identified as "critical" in Figure A.17, or in the top 10% of all three road network attributes of interest. Part b) shows identification of those road network facilities which experienced increases in both BC and SC under different tested Major Flooding Hazard Scenarios, shown in Figure 4.3. For example, a value of 1 indicates that BC and SC increased under only one scenario, while a value of 3 indicates that these increased in three different scenarios.

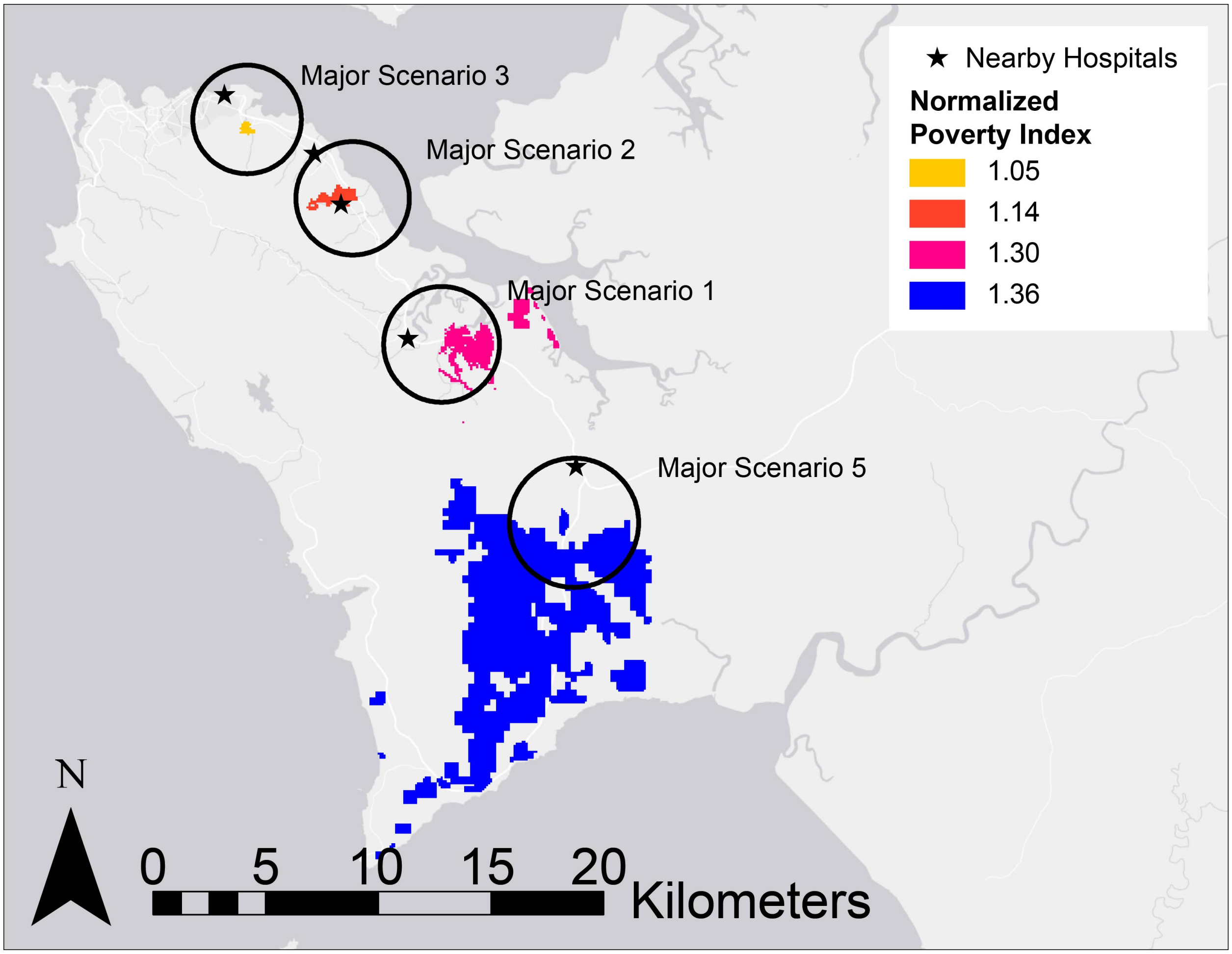

FIGURE 4.4: Normalized Combined Poverty Index averaged within zones experiencing decreases in hospital access under Major Hazard Scenario 1, 2, 3, and 5. Scenario 4, shown in Figure 4.3, is not featured because neighborhoods do not experience a shift in hospital accessibility in this scenario

Areas outlined in red in Figure 4.5.c highlight the road network facilities which are both critical to the system in terms of demand weight, SC, and BC and will have more importance during Major Flooding Hazard scenarios. Overlaps are simply determined by spatial coincidence. Transit routes that operate along these corridors represent important lifelines to people, particularly those who are low income and lack access to private transportation.

Following identification of critical areas, we return to the unique transit routes identified in supplemental Figure A.2. The spatial extent of these routes is positioned in comparison to the critical areas. However, the high variability in length and positioning of each route leads to large differences in their usefulness in both normal and hazard scenarios.

To illustrate this, the length of each route which coincides with the critical area is divided by its total length to calculate the percentage of its length which passes through the critical areas. This is illustrated in Figure 4.6 as "% Critical." Several poda poda routes on the Western coast are important in this regard, representing routes which present extra value beyond meeting daily commuting demand. Table 4.1 describes these routes in more detail.

The empty critical area extending south from the Waterloo additionally represents a missing

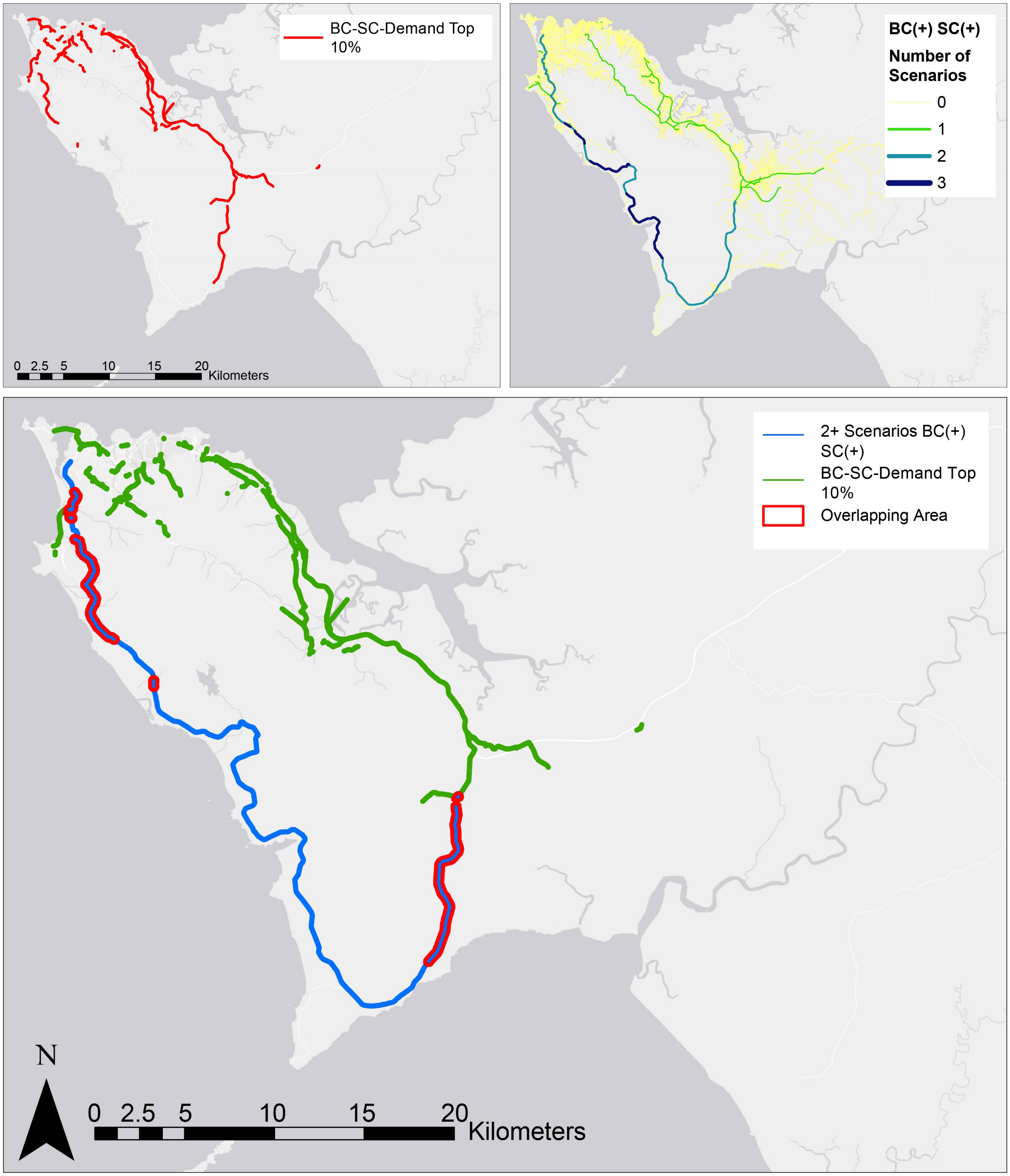

FIGURE 4.5: Selection process for critical road network areas: a) road network facilities in the top 10% percentile of both Demand Weight and SC (corresponding with Figure A.17 Critical category, red); b) road network facilities characterized by the number of Major Flooding Hazard scenarios which resulted in increases to BC and SC (corresponding with Figure 4.3 Demand(+) SC(+) category, blue); c) road network facilities which are indicated in both a) and the higher values (2 and 3) of b

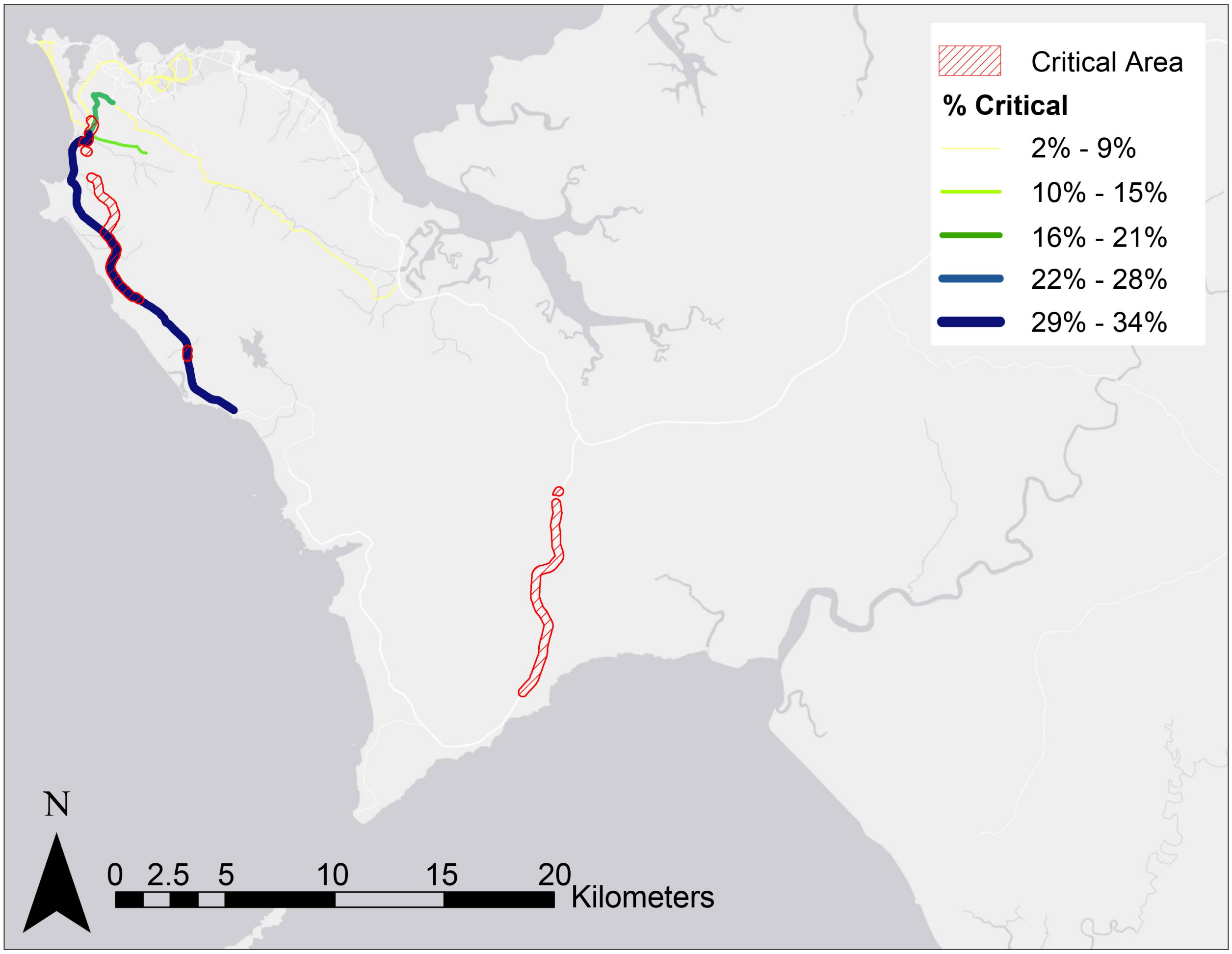

FIGURE 4.6: Transit routes categorized by the percent of their extent which passes through identified critical road network facilities

opportunity. Adding a route here would provide diverse benefit to local communities. Additionally, some transit connection between this area and the Western routes may add value to the system as a whole, particularly under emergency conditions. Poda podas with flexible routes that could be dispatched along this route specifically during natural hazard conditions may additionally add cost effective value for rural populations.

4.2 Effects of seasonal flooding hazards

Examining the effects of seasonal flooding hazards presented some difficulties - without more detailed traffic data, it was not feasible to accurately estimate the possible effects caused by localized obstacles, deep puddles, or muddy terrain on access by change in travel time.

Instead we sought to determine the overall exposure of each neighborhood's shortest path to its nearest facility to the possibility of these effects. We examined this by identifying the intersection of their unpaved portions with the seasonal flood extent. In this analysis, the Education SC becomes more important. With a higher incidence of facilities across the study area, Education SC is low throughout the system, reflecting the fact that no particular road is very important for most neighborhoods to access their nearest school, and that shifts to different facilities are unlikely to

TABLE 4.1: Transit Routes for Resilience

Mode	Route	Fare	Headway	% Critical
Poda Poda	Lumley to Baw Baw	3,000	18.5	34.3%
	Baw Baw to Lumley	3,000	19.8	33.3%
	Lumley to Ogoo Farm	1,500	13.4	30.3%
	Lumley to Wilberforce	2,000	8.9	19.7%
	Lumley to Kamayama	1,500	15.0	14.7%
	Regent Road to Lumley	1,500	14.6	8.2%
	Lumley to Regent Road	1,500	15.5	8.1%
	Kamayama to Lumley	1,500	7.7	5.8%
	Lumley to Jui	5,000	12.7	2.7%
Taxi	Ogoo Farm to Lumley	1,500	12.0	28.9%
	Wilberforce to Lumley	2,000	6.9	20.5%
	Lumley to Aberdeen Village	1,500	11.7	4.1%
	Jui to Lumley	5,000	12.7	3.5%
	Aberdeen Village to Lumley	2,000	10.8	2.7%

result in large increases in travel distance. Therefore, access to schools in general is unlikely to be affected by major disasters. However, SC becomes an important proxy for the roads within a single service area that might benefit the most from improvement. From the viewpoint of individual neighborhoods, certain neighborhoods' path to their nearest school may be largely unpaved, leading to difficult or unsafe conditions during seasonal rain conditions. Certainly, there is a difference in this regard between neighborhoods and even between service areas.

Figure 4.7 shows the process undertaken to examine this idea, with 4.7a showing the intersection of roads important to accessing a senior secondary school with the flood risk extent. Figure 4.7b translates this into the percent of each road segment which intersects with seasonal flood risk areas. Finally, 4.7c aggregates this to each neighborhood's shortest path, calculating the percent of the shortest path that is vulnerable to seasonal events and applying it to each neighborhood. It is evident that certain neighborhoods have an advantage over others in their commute to their nearest facility, due to a combination both of geography and road quality. As shown in the southern neighborhoods of 4.7c, even neighborhoods that are physically close to their nearest facility may have the highest vulnerability for their shortest paths. These areas may represent populations which are vulnerable in other ways as well, so using this data in conjunction with the availability of other demographic information could help add an equity focus to improvement projects of transportation infrastructure.

This concept is also easily applicable at the Service Area level by similarly calculating the percent of all shortest paths that are unpaved and exposed to seasonal flooding. Figure 4.7d shows this process undertaken among the Top 10 largest service areas for senior secondary schools.

Additionally, we applied the poverty index averaging method described in the Effects of Major Flooding Hazards section, above, to the same Service Areas in Figure 4.7e. The side-by-side comparison of these two visualizations shows that exposure to seasonal weather conditions and poverty are correlated, with the highest percentage of vulnerable shortest paths coinciding with poverty score. Using these methods, areas of investment can be identified which not only improve accessibility for large populations, but also serve the populations which are most vulnerable to poverty first.

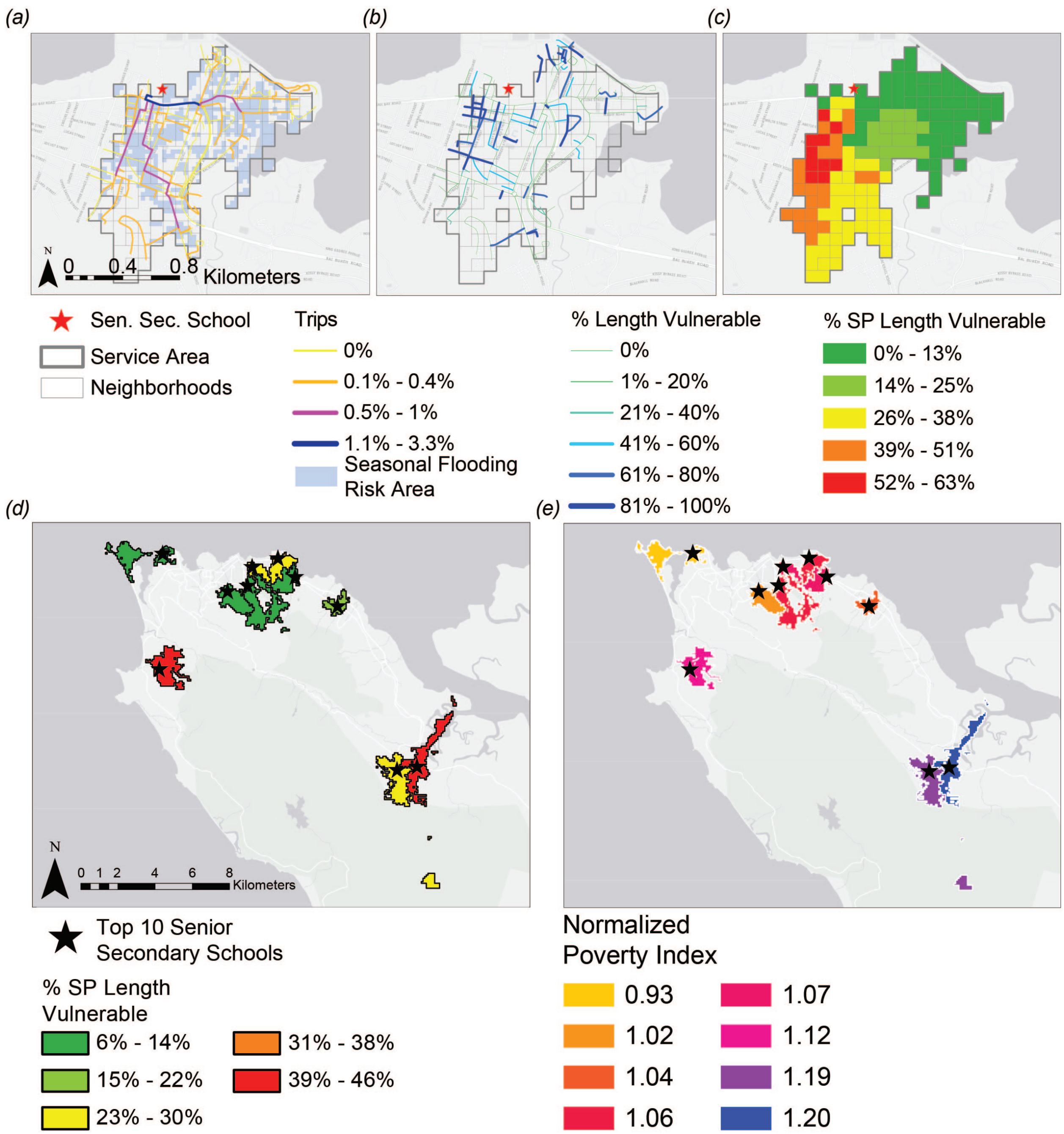

FIGURE 4.7: Seasonal Flooding Risk in the top Senior Secondary School Service Areas: a) SC of roads for Senior Secondary School access compared to extend of seasonal flooding risk area; b) extent of vulnerability of unpaved roads to seasonal flooding, c) Extent of vulnerability to seasonal flooding per neighborhood shortest path, d) Seasonal vulnerability of shortest paths per service area, e) Normalized Combined Poverty Index, averaged over each service area

Chapter 5

Conclusion

This work links road network analysis to accessibility and facility demand, allowing us to quantify the broader effects of climate events on various populated areas. We compared the effects of likely scenarios in different areas as a way to inform and compare the potential impact of infrastructure investments. In addition, we used a network metric, service centrality (SC), which can be tailored to any specific facility or combination of facilities, incorporating any number of co-benefits, to improve accessibility to a targeted facility type or a variety of services.

These concepts were applied at different scales, from the zoomed-out system view for major flooding hazards to individual service areas for seasonal hazards. Varying levels of specificity and application speak to a highly generalizable concept with applications to a variety of needs. With data and processing largely relying on publicly available sources, these findings offer a flexible method to planners or governments at various development levels who are interested in maximizing co-benefits to transportation investments.

5.1 Recommendations

Candidates for infrastructure hardening were identified as the nodes eliminated during Major Hazard Scenarios. A comparison of the resulting decrease in Demand Weight and SC in these scenarios can help government and lending institutions identify targets which will provide a maximum benefit for cost. Similarly, examining these decreases in concert with poverty indicators allows consideration of who would benefit from improvements. Poverty risk at the regional level might decrease the most by improving conditions for the most vulnerable.

Candidates for transit service improvement were identified as the streets which saw the greatest increase in Demand Weight and SC during Major Hazard scenarios. Improving transit options along these corridors would reduce vulnerability to disruptive events by preventing the increase in travel time to facilities from becoming overly onerous. Adding transit connectivity in identified missed opportunity areas would be an added benefit, depending upon the cost of providing such a service.

Additional hardening projects that would provide a great benefit is paving dirt roads. We identified candidates for these types of improvements through Seasonal Hazard analysis. Facility Service Areas which had the highest percentage of unpaved shortest paths and the highest average poverty indicators would benefit the most from such improvements.

There are also many opportunities to continue this study in the future. We were fortunate to have access to travel demand data, which allowed for more accurate approximations of general network connectivity than traditional betweenness centrality. However, we must also consider that the level of usage of mobile phones in a developing nation is difficult to ascertain, particularly among groups of different economic levels. Therefore, this study would also be improved by conventional trip data in addition to more accurate environmental data, precipitation gauges and river flow data. We understand that the expense of such studies is likely prohibitive.

Overall, we hope to encourage the combination of various data sources to generate metrics that help the assessment of development strategies. In a time that is increasingly rich with open or low-cost data sources, these methods present an opportunity for developing nations to not only take advantage of information, but develop institutional capacity through learning and experimentation.

Freetown and Sierra Leone in particular stand to benefit from increasing such capacity. Sierra Leone's current decentralized governance system should be respected after its conflict-ridden post-colonial history. However, institutions like the World Bank are in a unique position to be able to inspire coordination and coalition-building between local governments and Federal institutions. By inspiring stakeholders at various levels to work together, data analysis methods such as these can help create local capacity and knowledge, building invaluable social capital in the long-term. We hope that this can help guide cities as they develop, with individual improvements generating ripple effects through interconnected urban systems.

Appendix A

Supplemental Figures

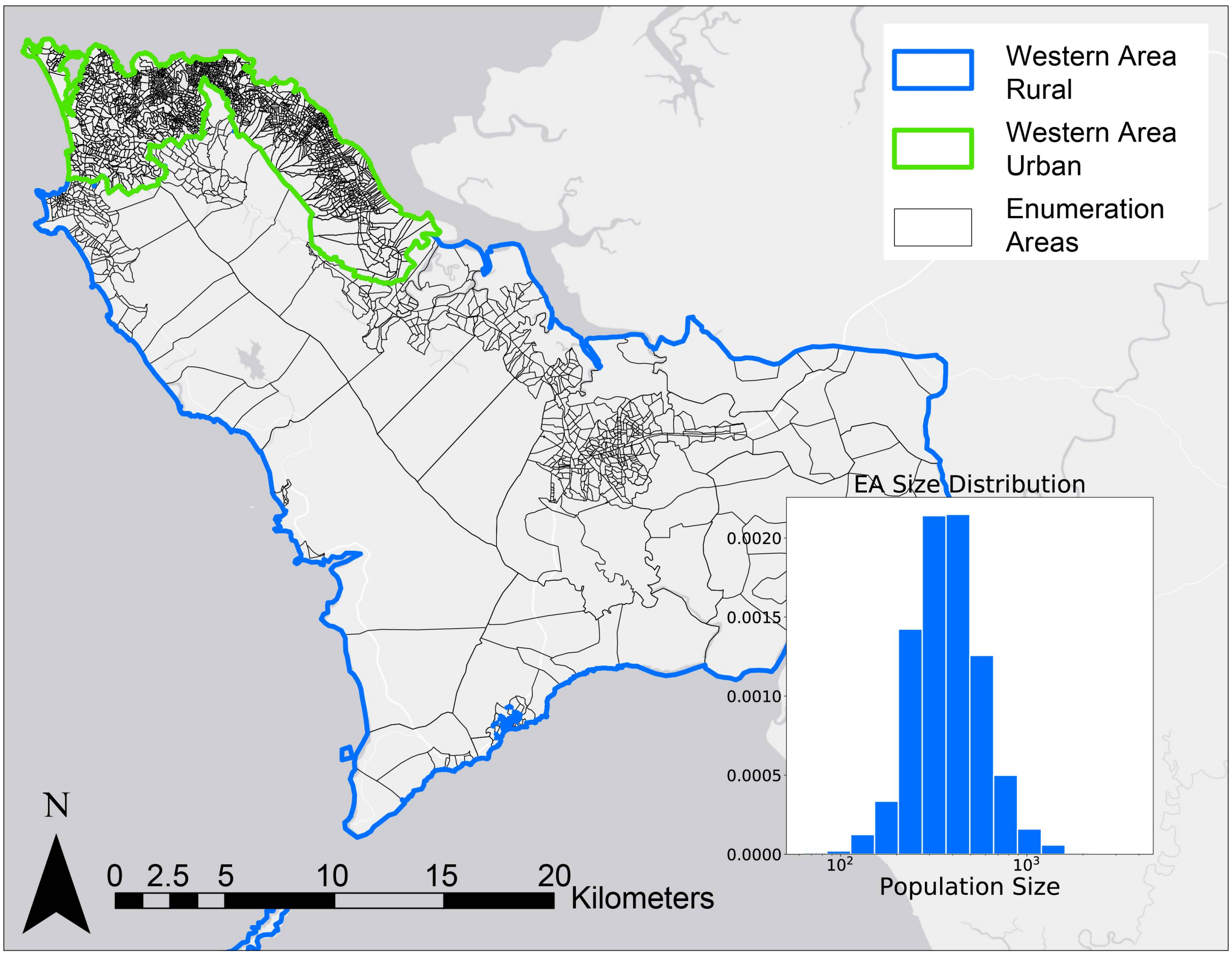

FIGURE A.1: Freetown Peninsula Enumeration Areas and Population Distribution (inset)

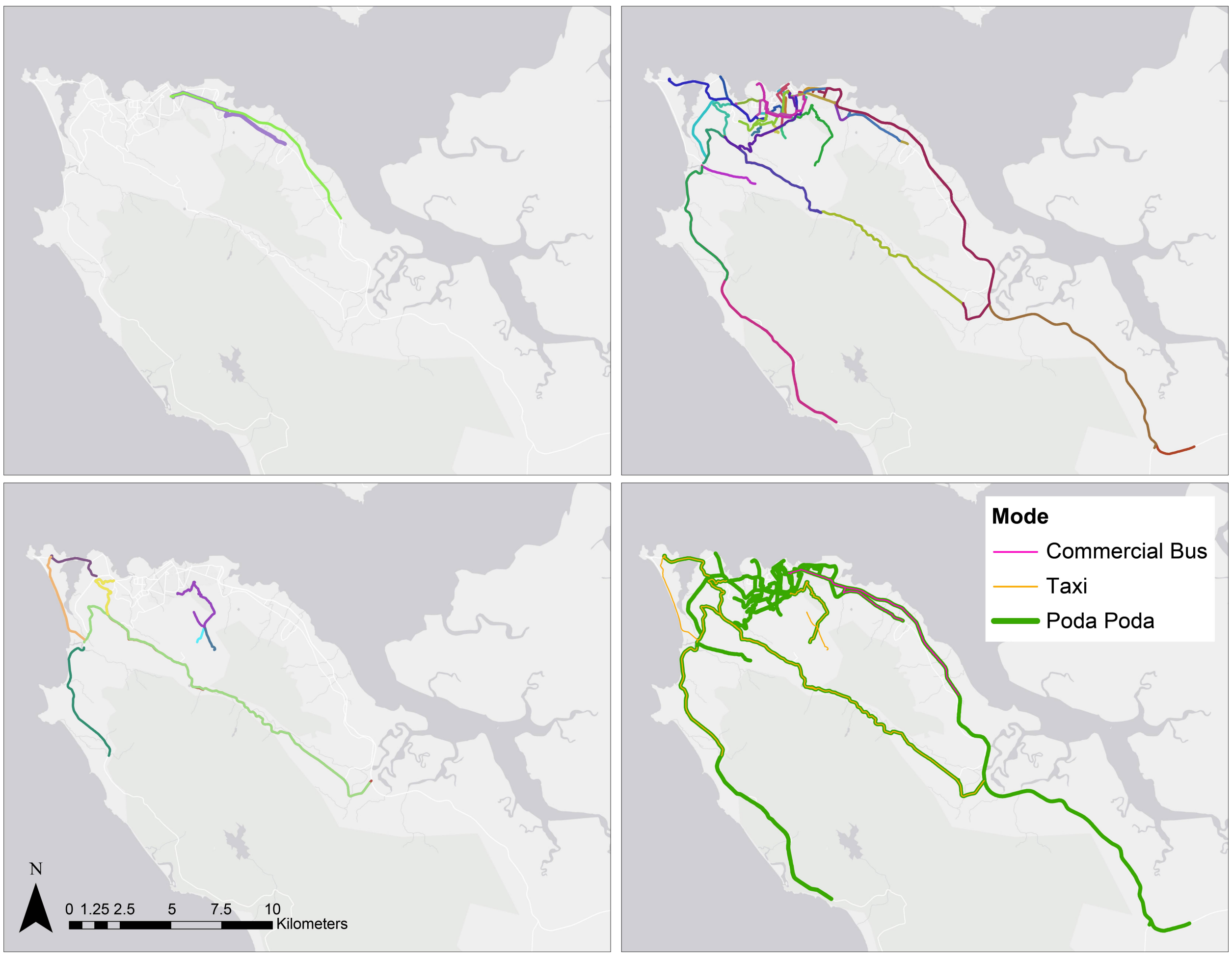

FIGURE A.2: Spatial extent of unique routes for commercial bus (upper left); poda poda (upper right); taxi (lower left); spatial extent of all modes (lower right)

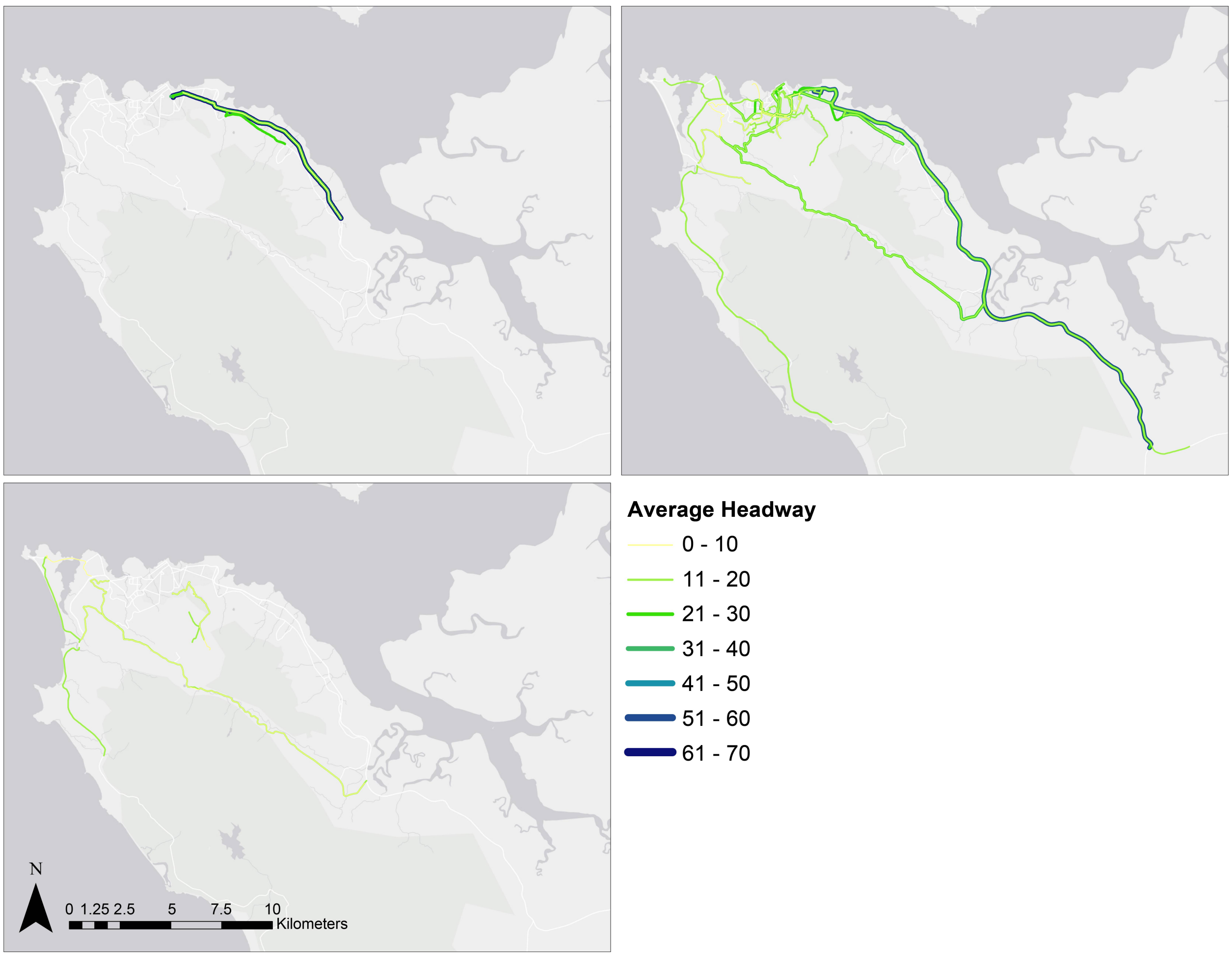

FIGURE A.3: Average headway (minutes) for commercial bus routes (upper left), poda poda routes (upper right), taxi routes (lower left). Commercial bus routes have the longest headways, while poda poda routes occupy middle categories and taxi routes have the shortest

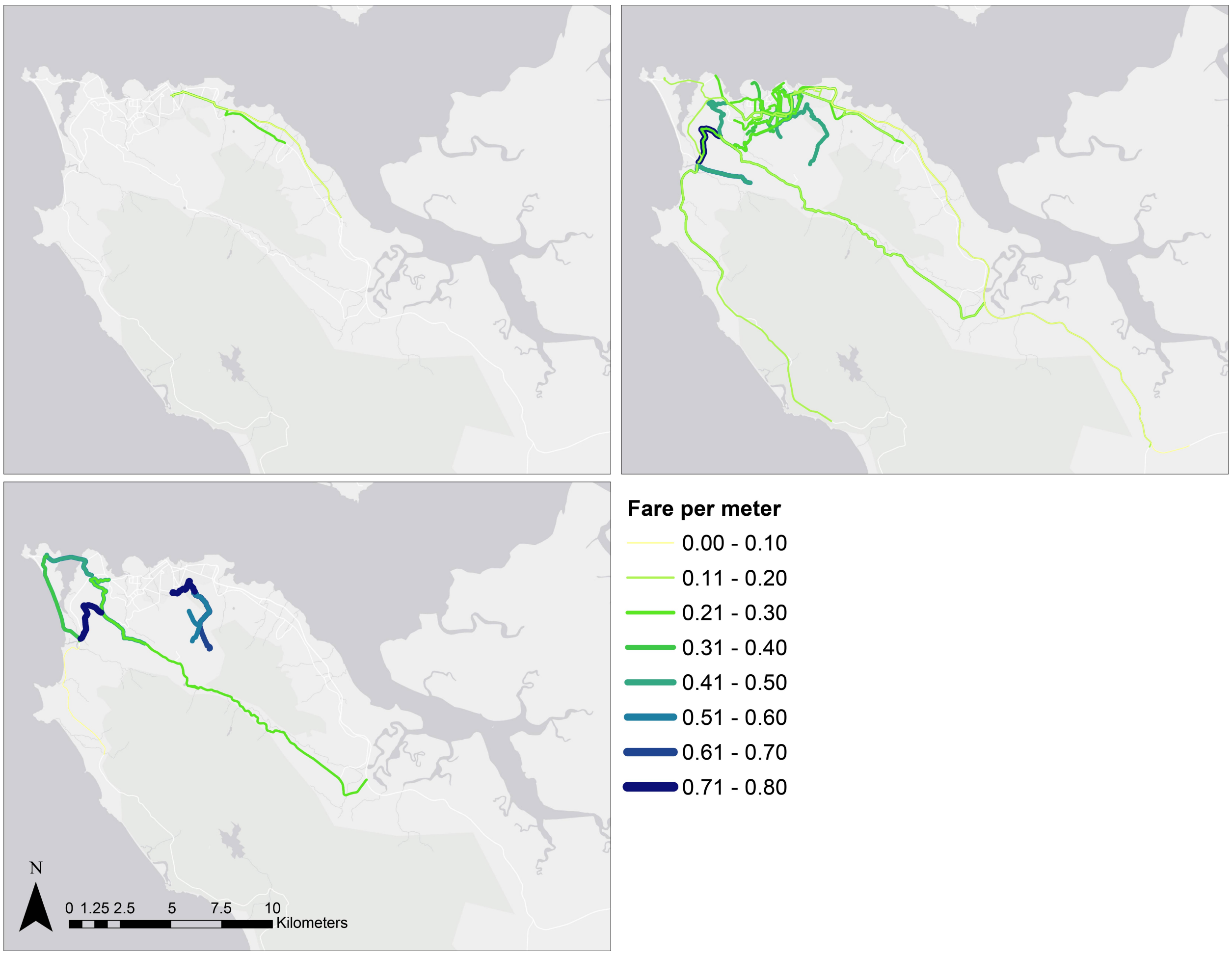

FIGURE A.4: Average fare, normalized by distance (meters) for commercial bus routes (upper left), poda poda routes (upper right), taxi routes (lower left). Commercial buses have the lowest fares, while poda poda routes represent the middle categories and taxis are the most expensive.

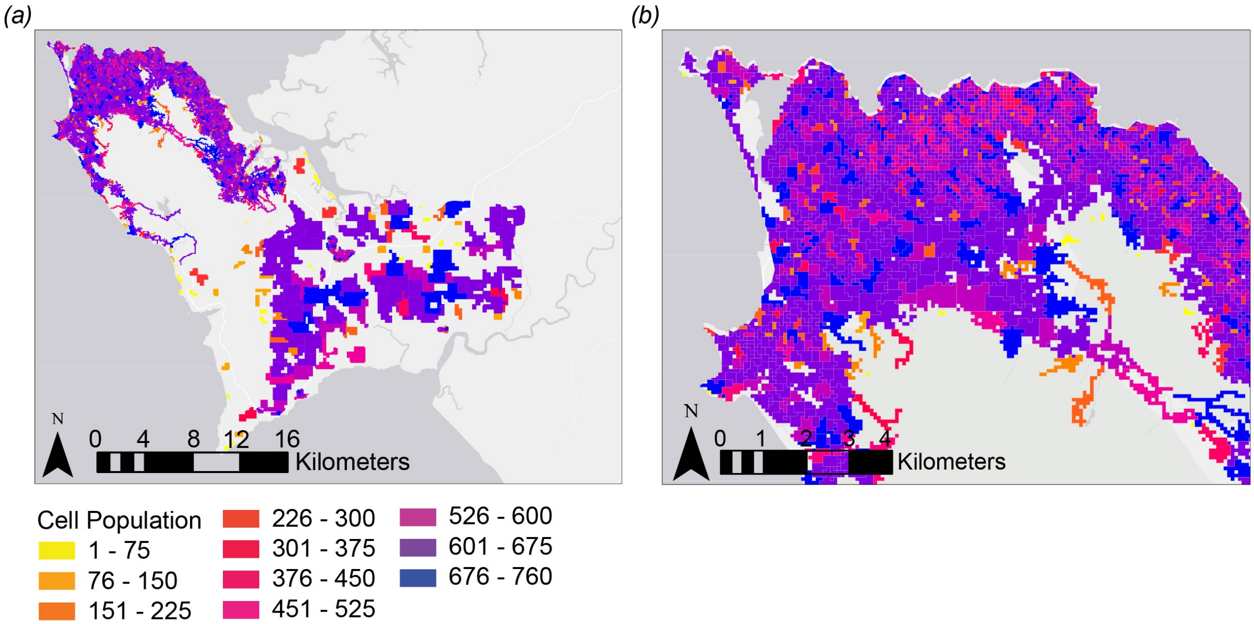

FIGURE A.5: Method: Neighborhood Generation, a) Neighborhood population size; b) Freetown CBD detail

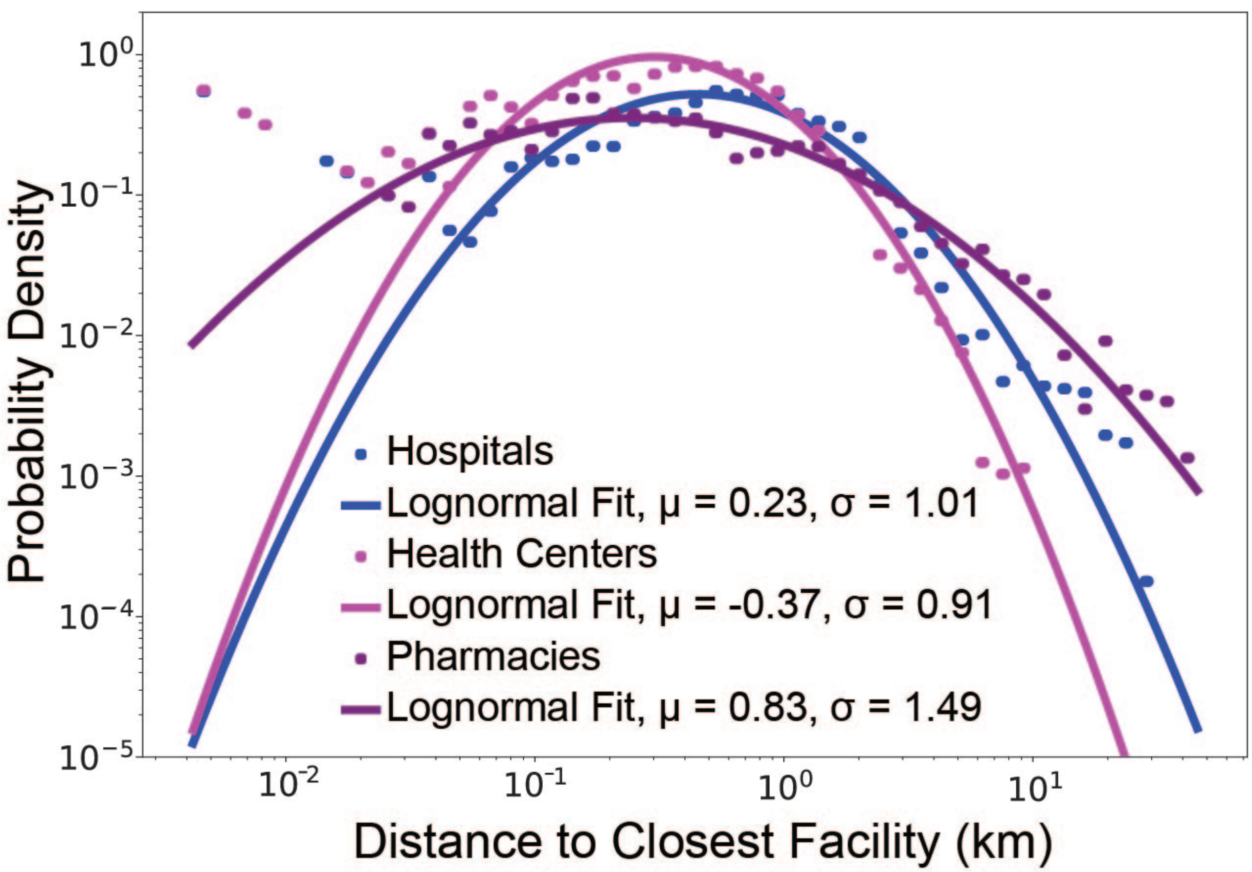

FIGURE A.6: Neighborhood Generation and Accessibility Calculation: Distribution of neighborhood distance to health facilities

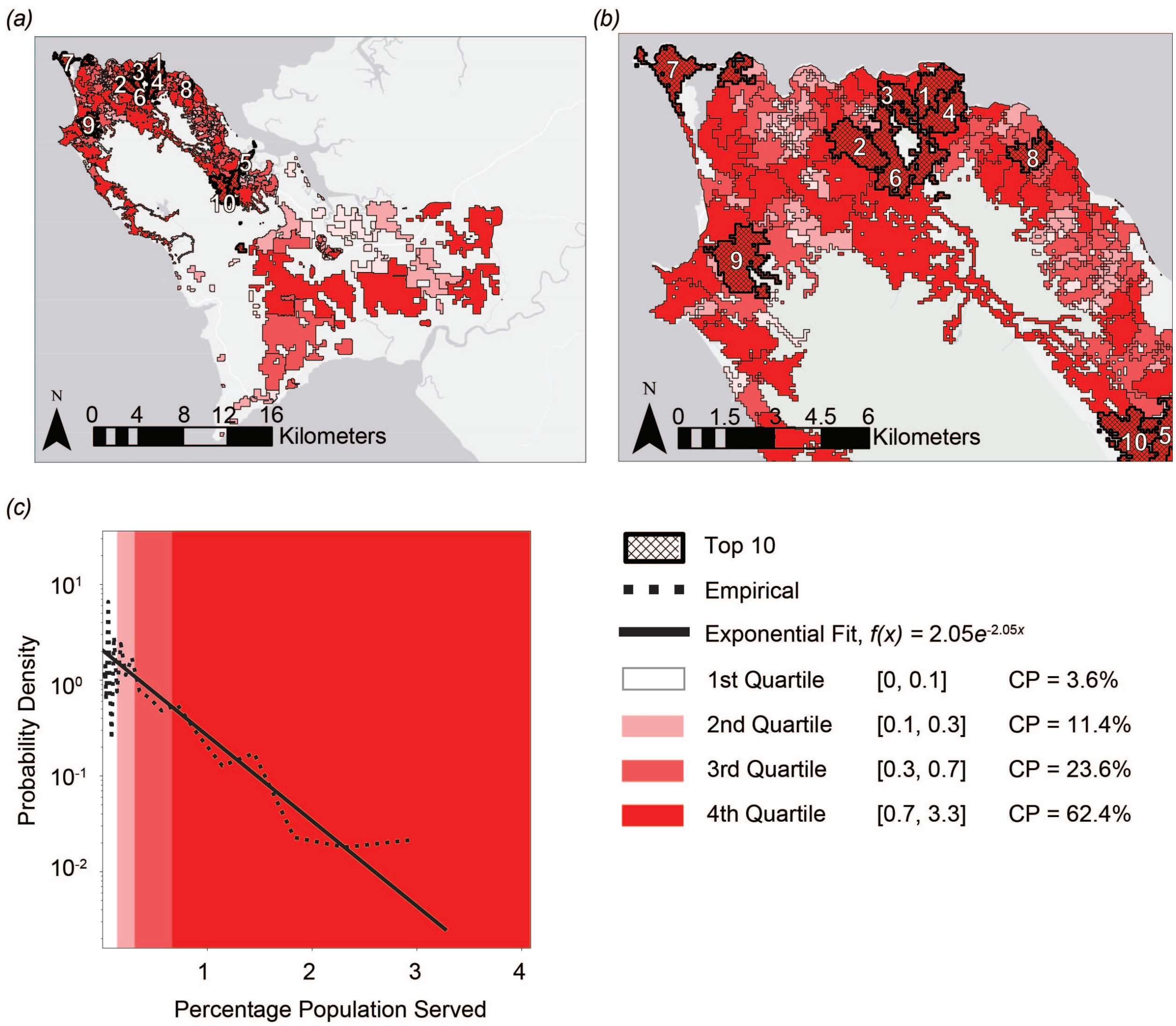

FIGURE A.7: Demand Distribution: a) Senior Secondary Schools (n = 208); b) Freetown Central Business District Detail; c) Distribution with fit

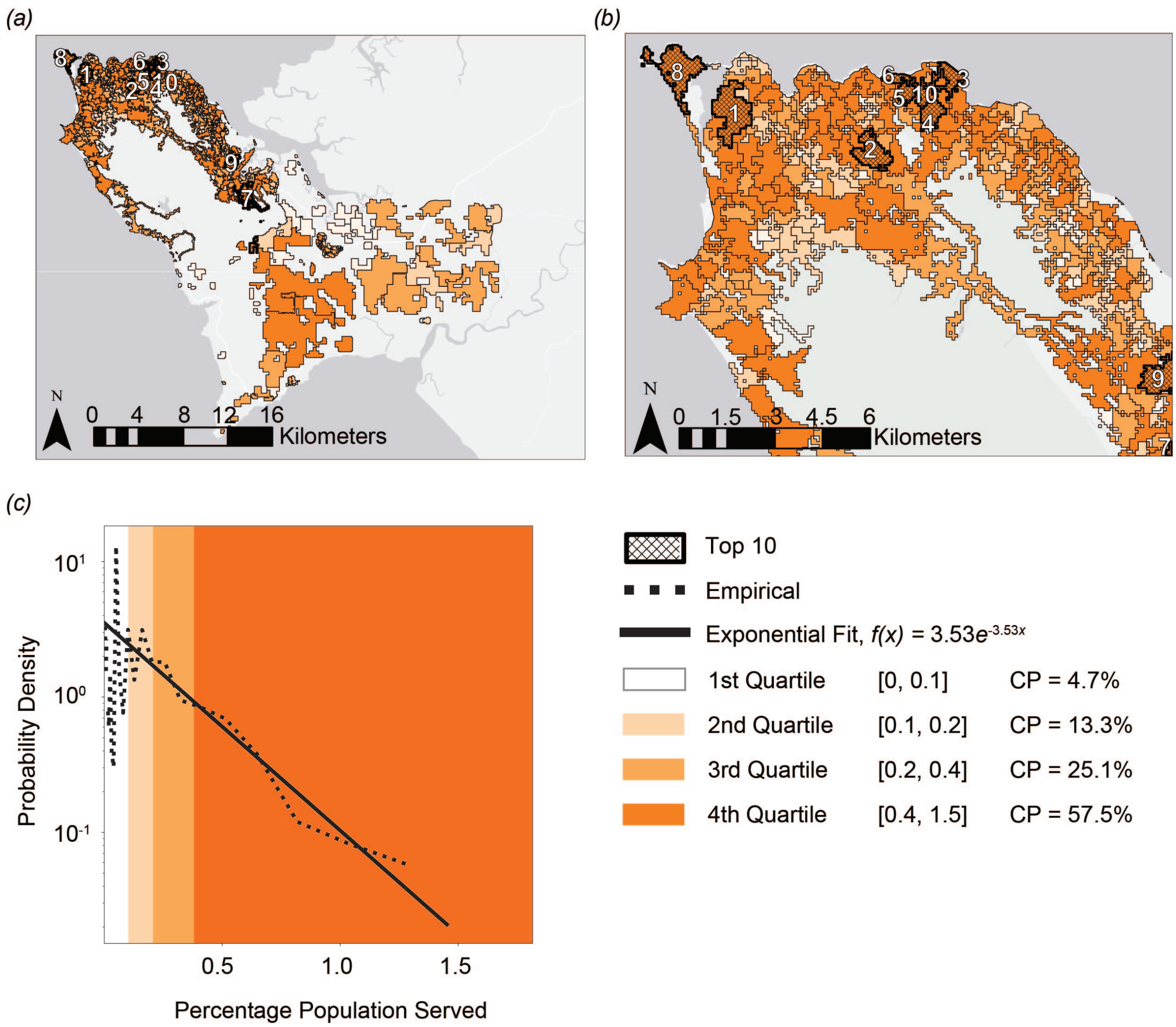

FIGURE A.8: Demand Distribution: a) Junior Secondary Schools (n = 353); b) Freetown Central Business District Detail; c) Distribution with fit

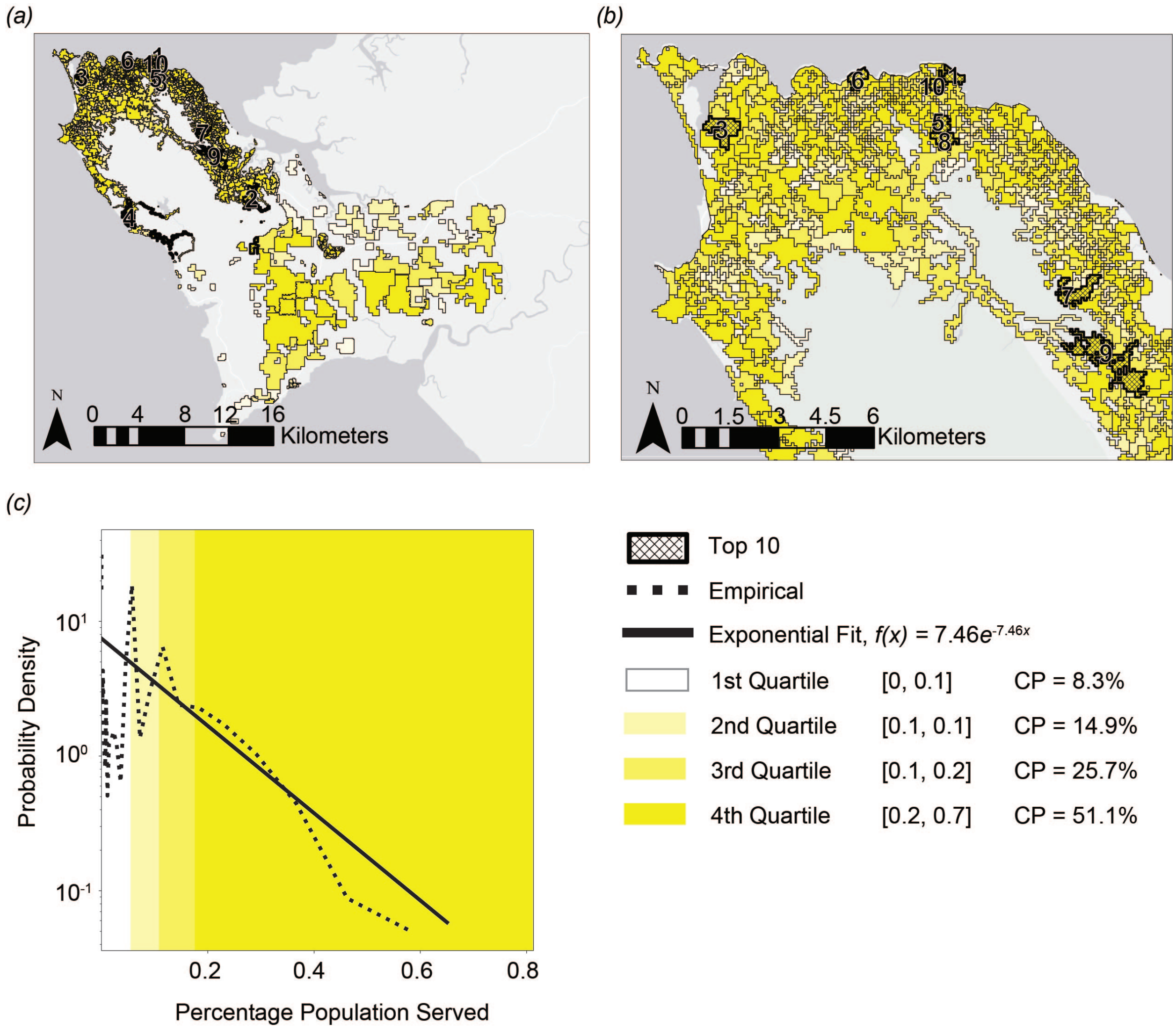

FIGURE A.9: Demand Distribution: a) Primary Schools (n = 746); b) Freetown Central Business District Detail; c) Distribution with fit

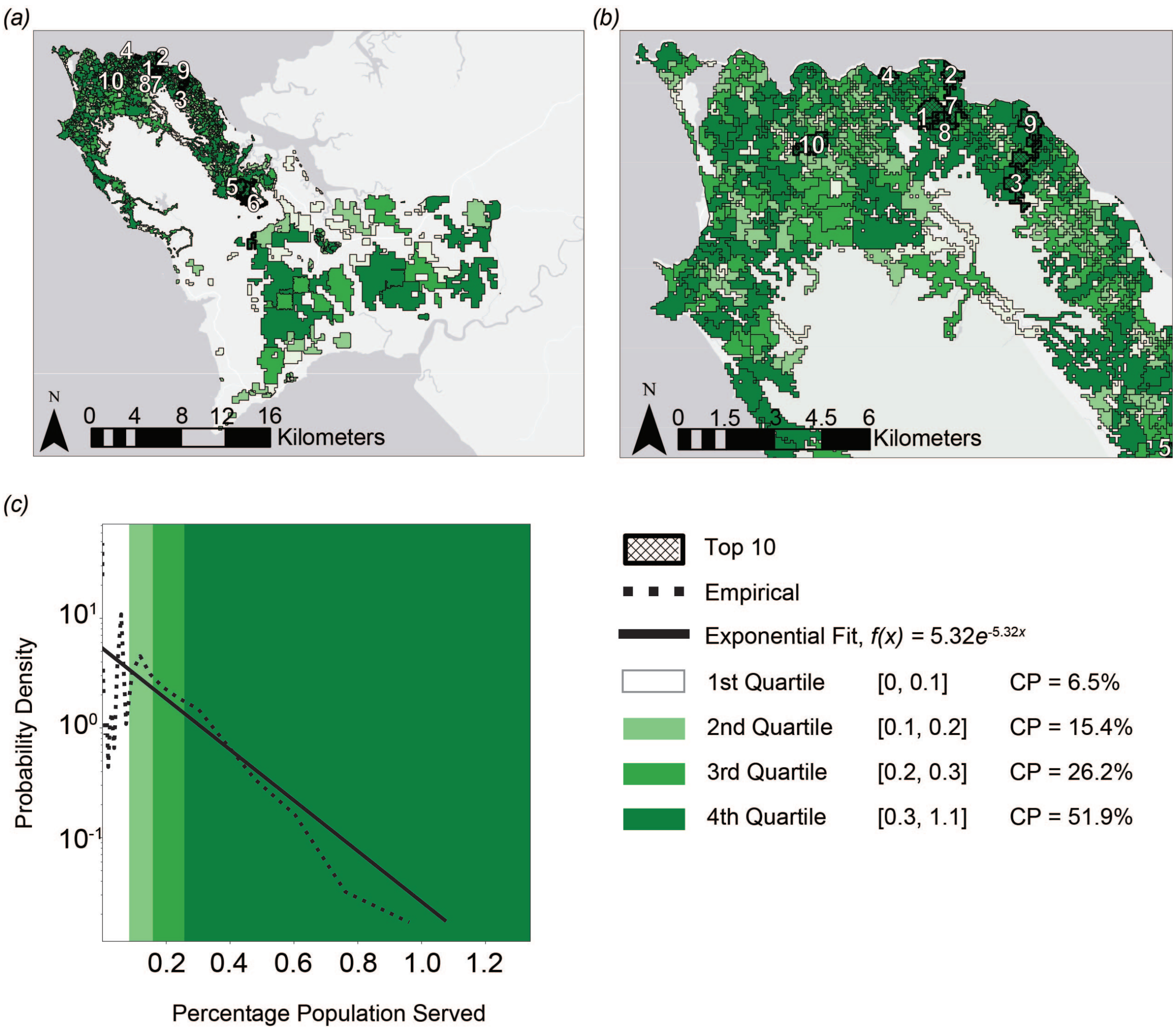

FIGURE A.10: Demand Distribution: a) Pre-Primary Schools (n = 532); b) Freetown Central Business District Detail; c) Distribution with fit

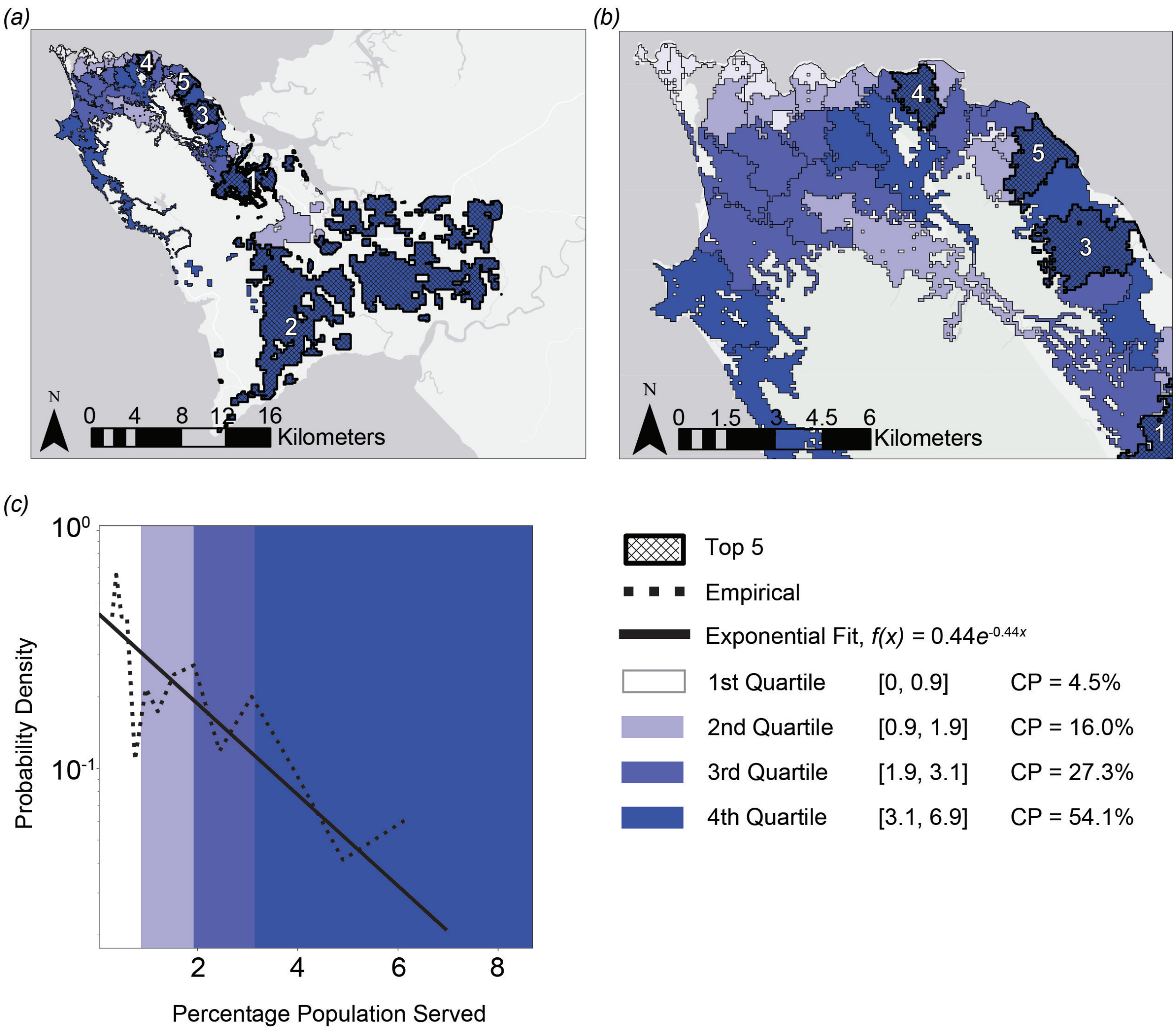

FIGURE A.11: Demand Distribution: a) Hospitals (n = 44); b) Freetown Central Business District Detail; c) Distribution with fit

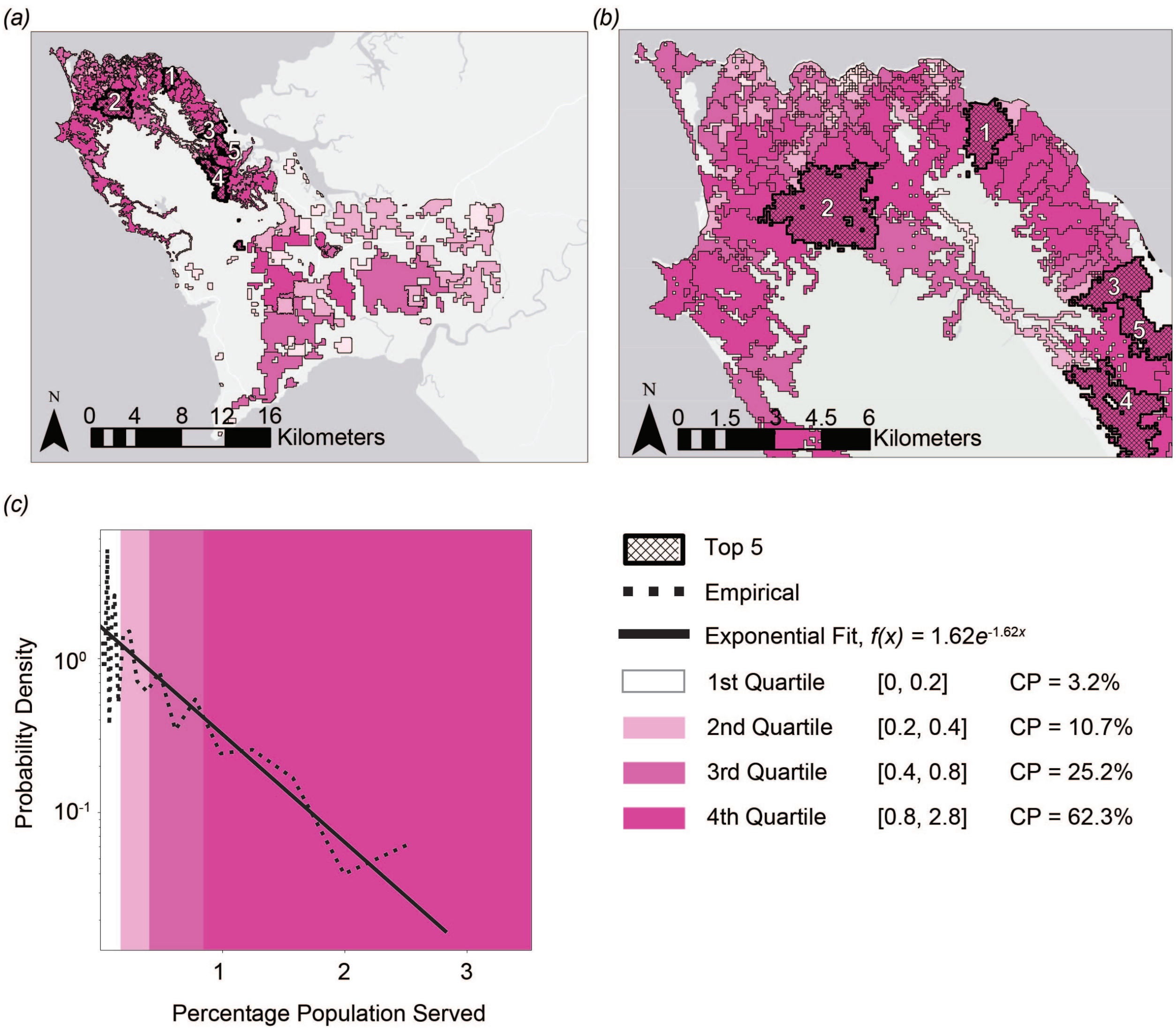

FIGURE A.12: Demand Distribution: a) Health Centers (n = 164); b) Freetown Central Business District Detail; c) Distribution with fit

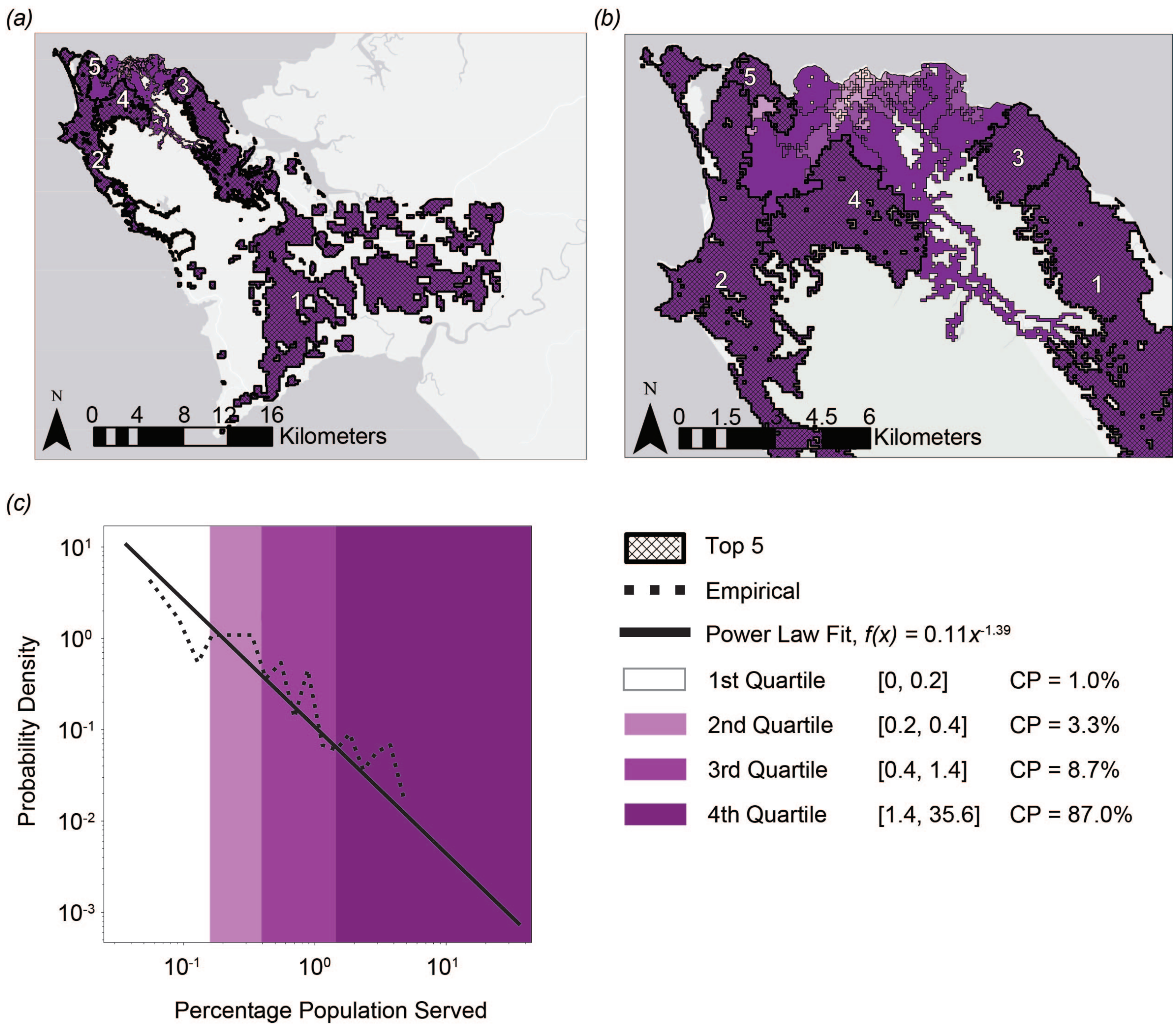

FIGURE A.13: Demand Distribution: a) Pharmacies (n = 50); b) Freetown Central Business District Detail; c) Distribution with fit

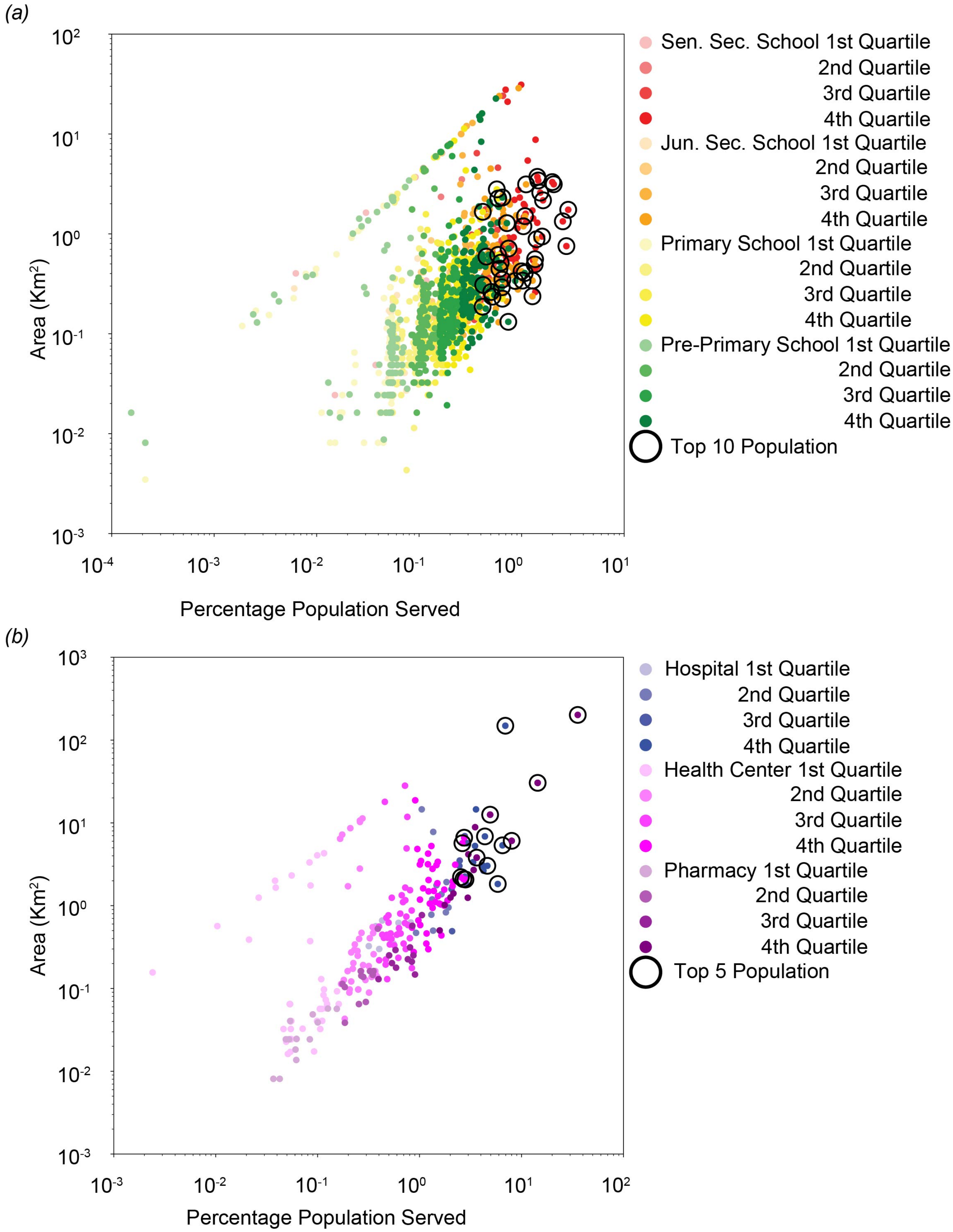

FIGURE A.14: Demand, Size of service areas compared to population served: a) Education facilities; b) Health Facilities

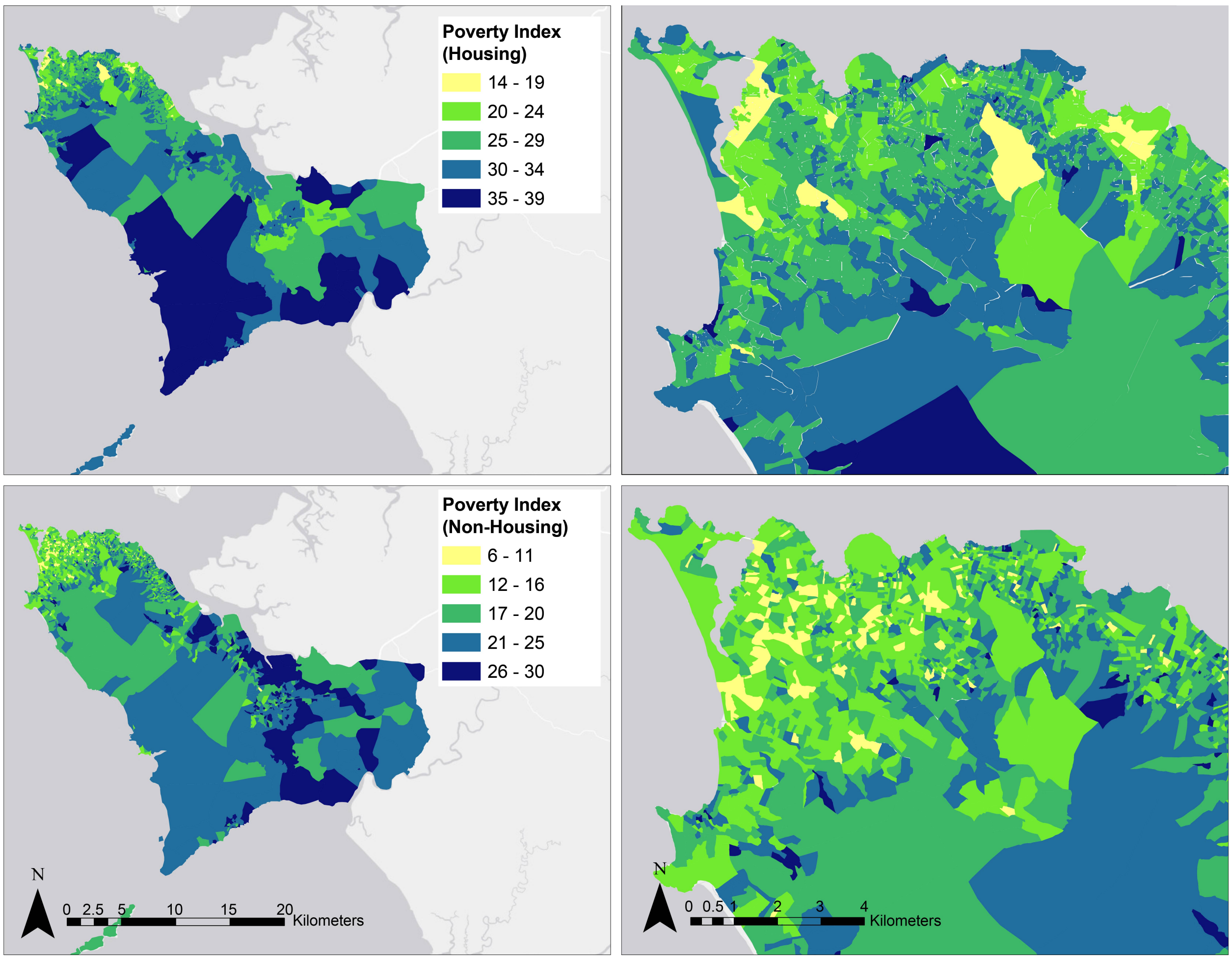

FIGURE A.15: Poverty index for housing factors (top left, top right) and non-housing factors (bottom left, bottom right)

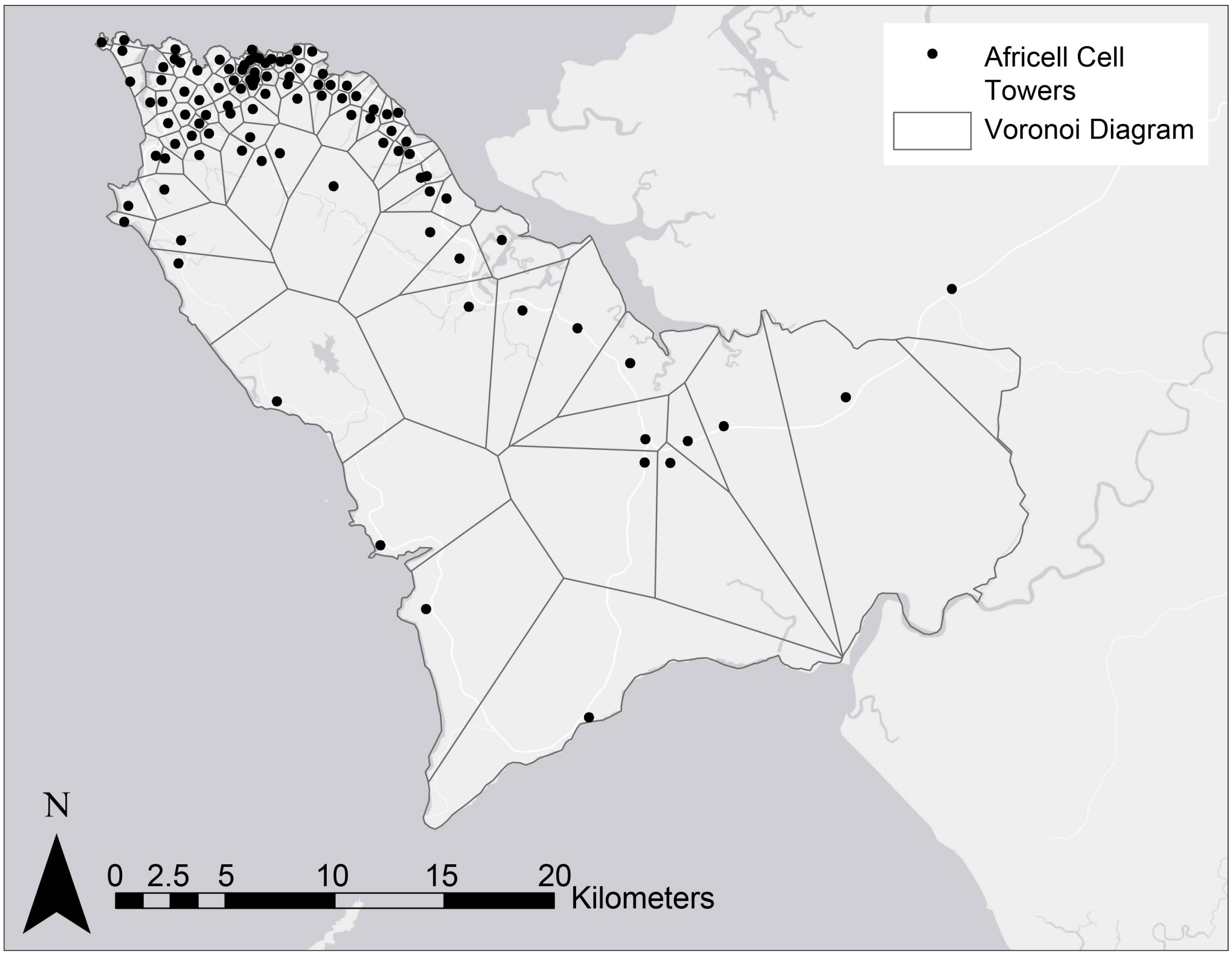

FIGURE A.16: Freetown Peninsula partitioned into a Voronoi diagram by Africell cell tower location

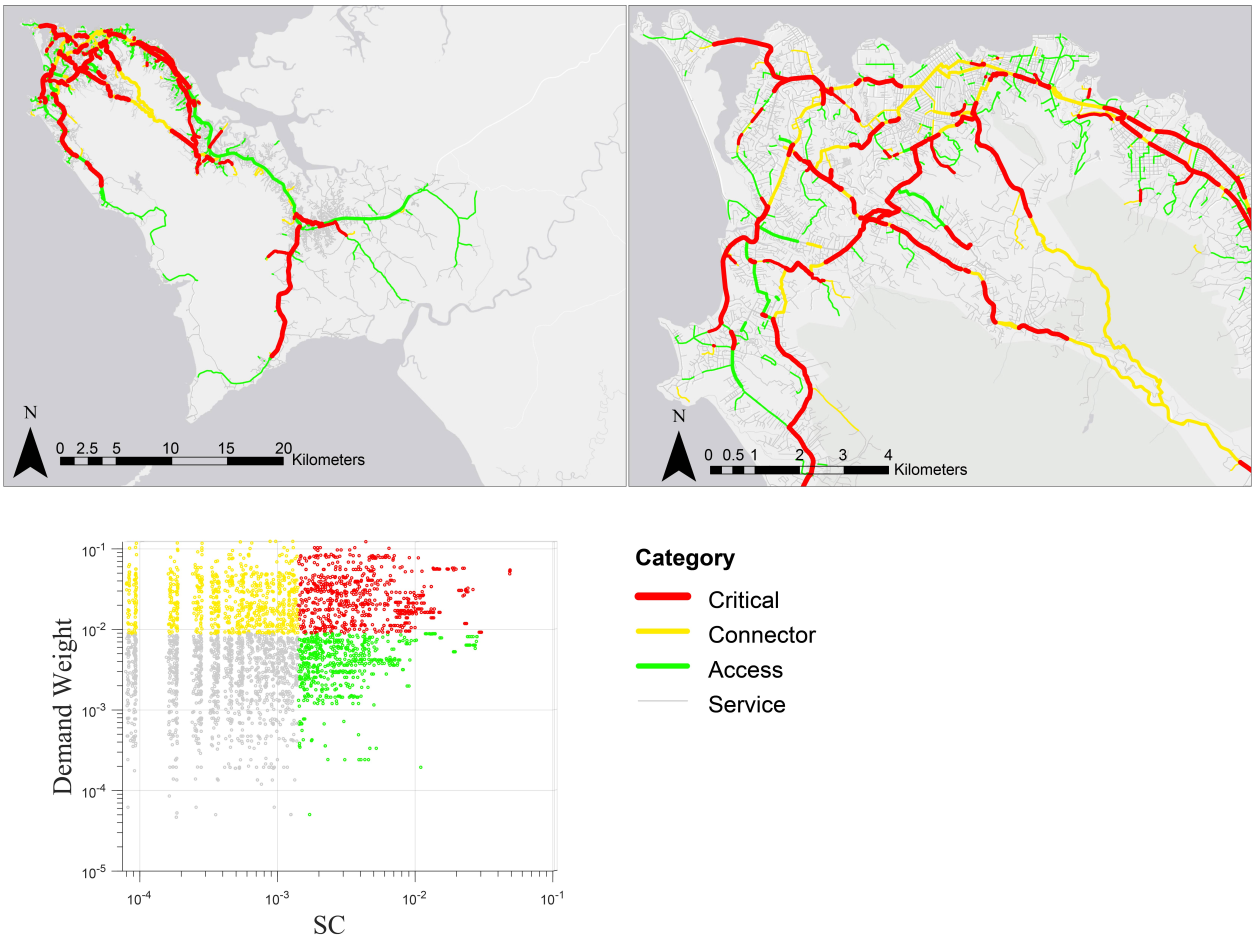

FIGURE A.17: Combining Service Centrality and Demand Weight in the road network allows road segments to be categorized by anticipated usage. Considering road segments with values above the 90th percentile in Demand weight and SC creates: a) road categories in Western Area Urban and Western Area Rural; b) Freetown CBD detail; c) scatterplot of service centrality and edge betweenness centrality of network edges

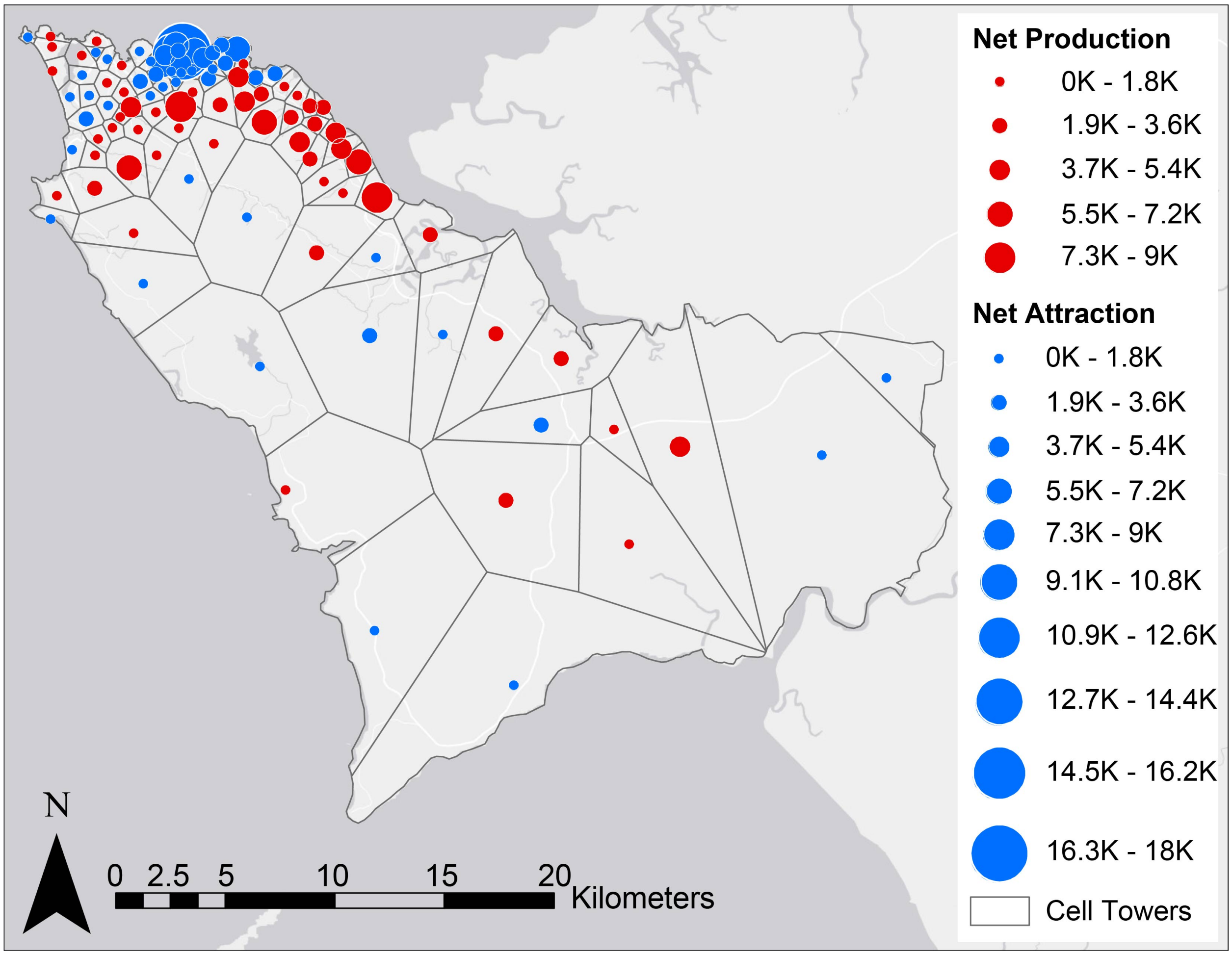

FIGURE A.18: Net trip production and attraction set within a Voronoi diagram based on cell tower location shows likely job attraction areas (North, blue dots) and residential production areas (Northeast coast, red dots)

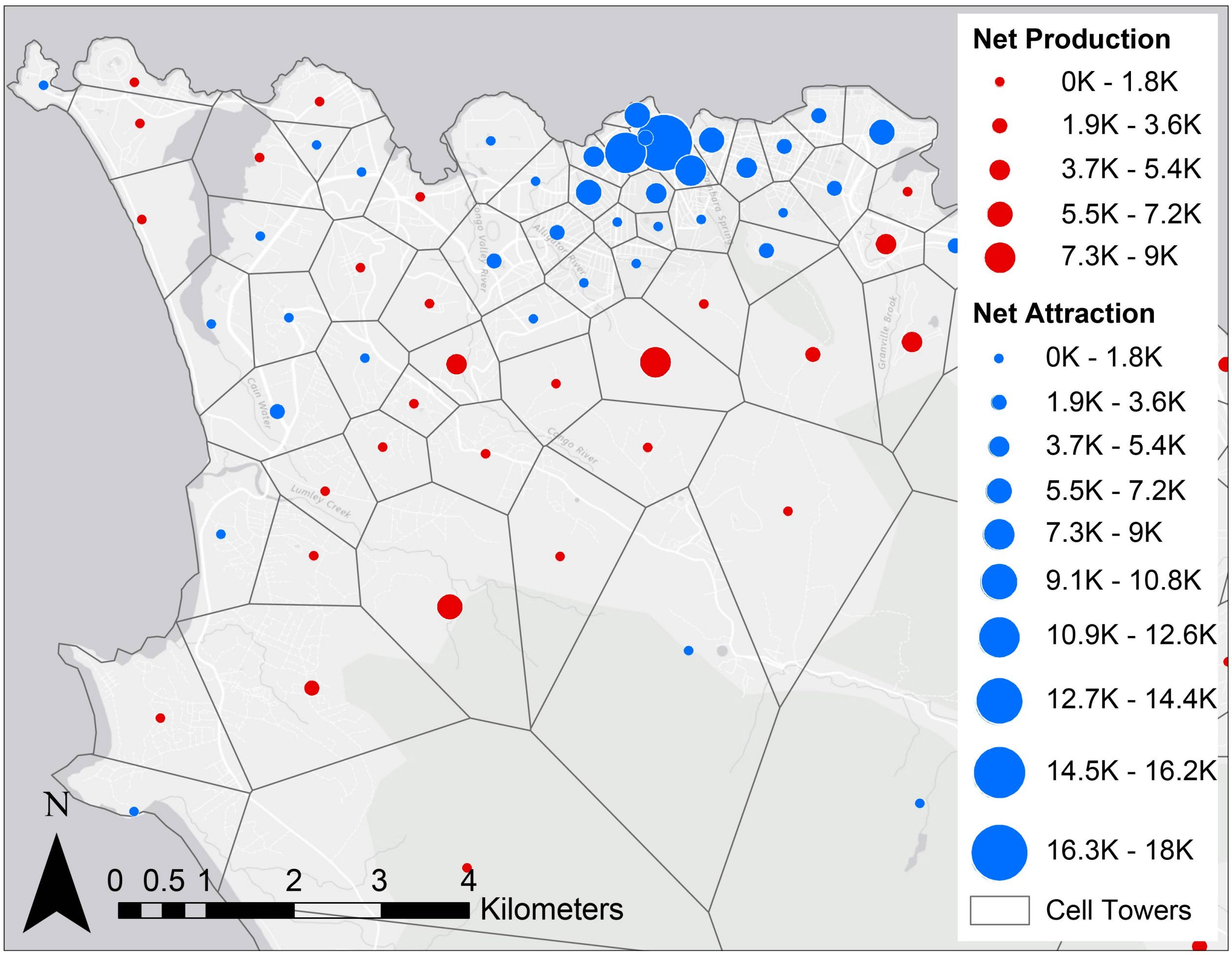

FIGURE A.19: Jobs are likely to be highly concentrated in Tower Hill, with some spillover into directly surrounding neighborhoods. The Wilberforce and Lumley areas to the West also serve to attract trips.

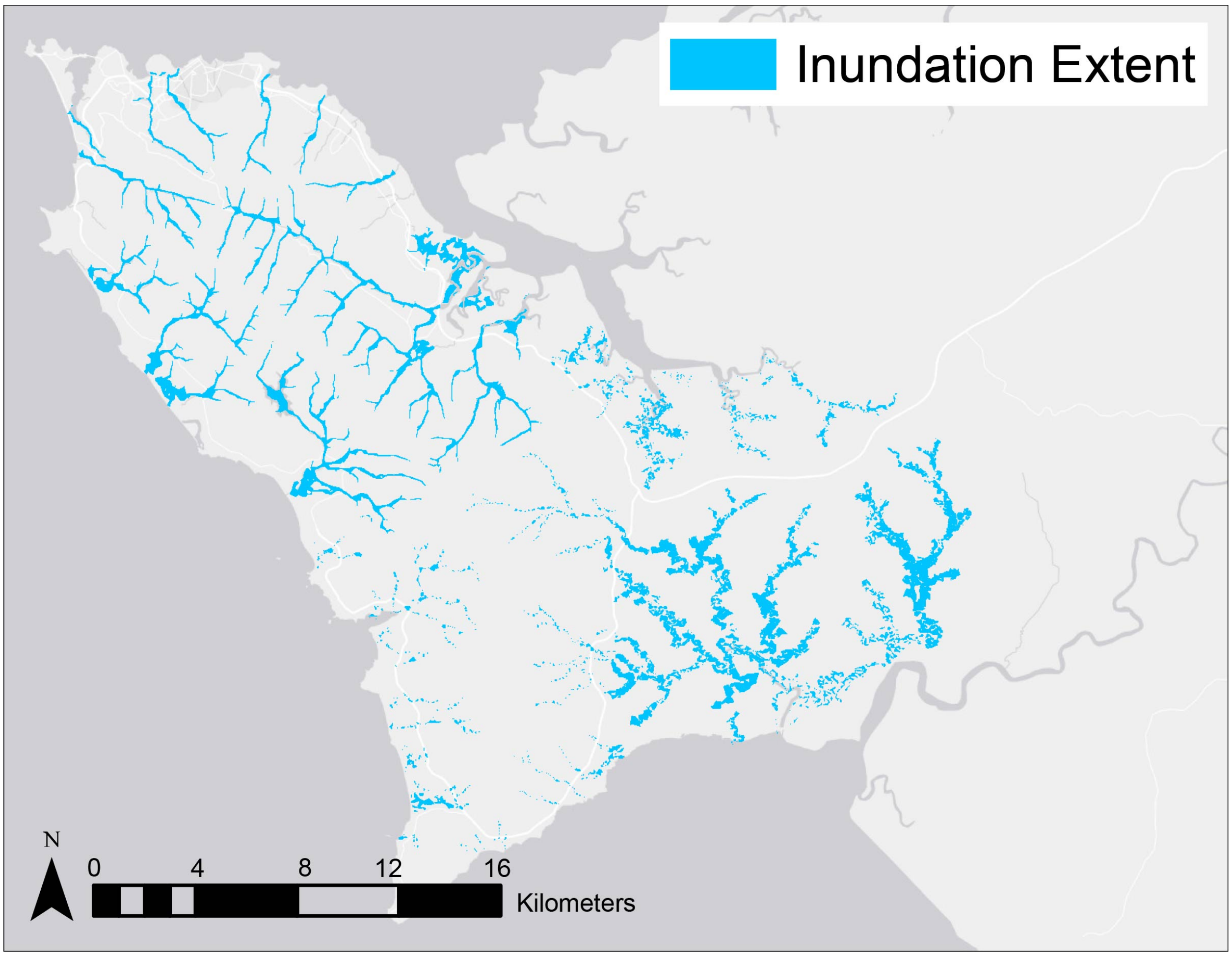

FIGURE A.20: Major Flooding Hazard Extent

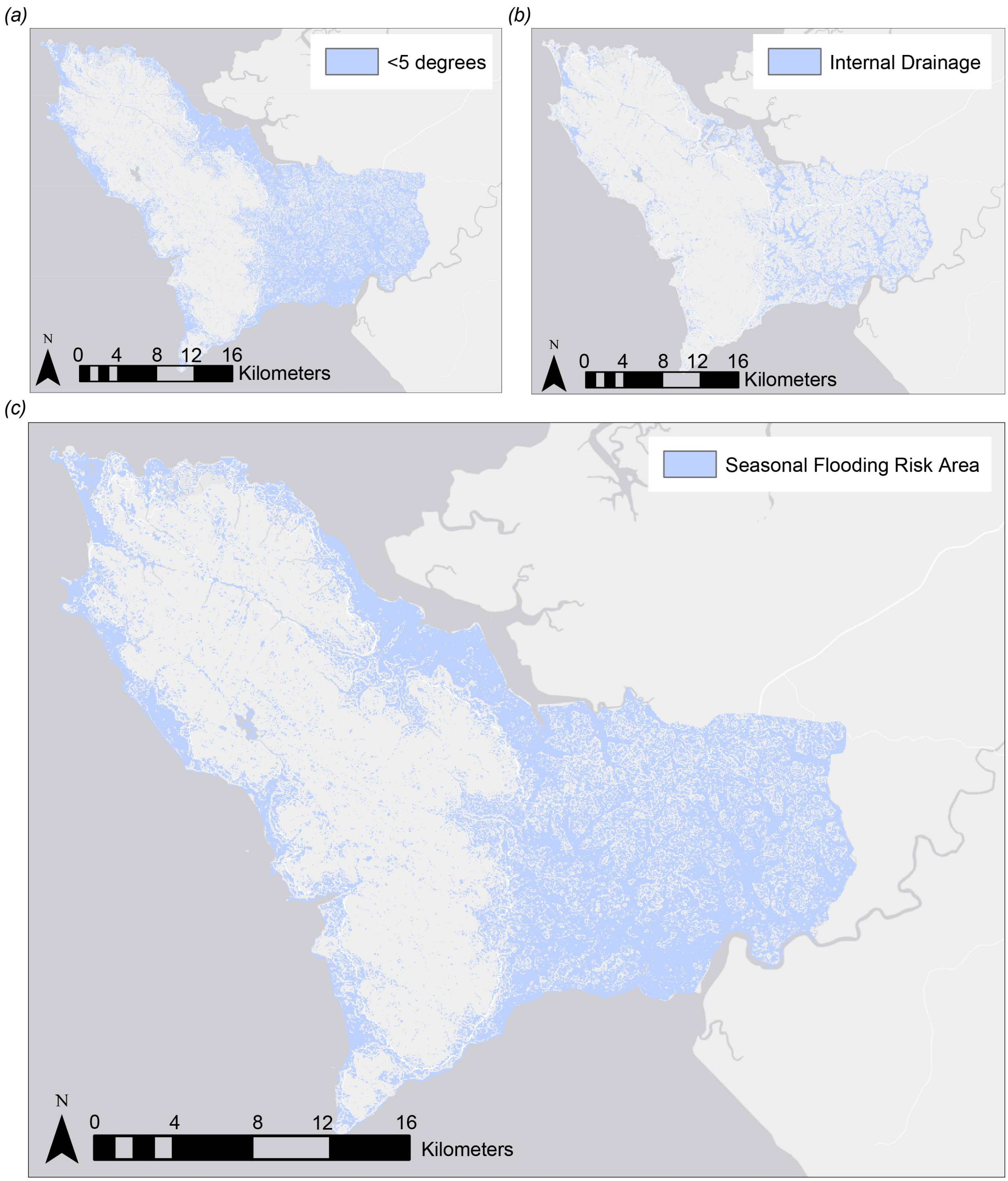

FIGURE A.21: Seasonal Flooding Hazard Extent, a) Areas with slope of less than five degrees; b) Sinks, or areas with no outlet for drainage, c) Union of 11a) and 11b), representing the extent of expected seasonal flooding risk

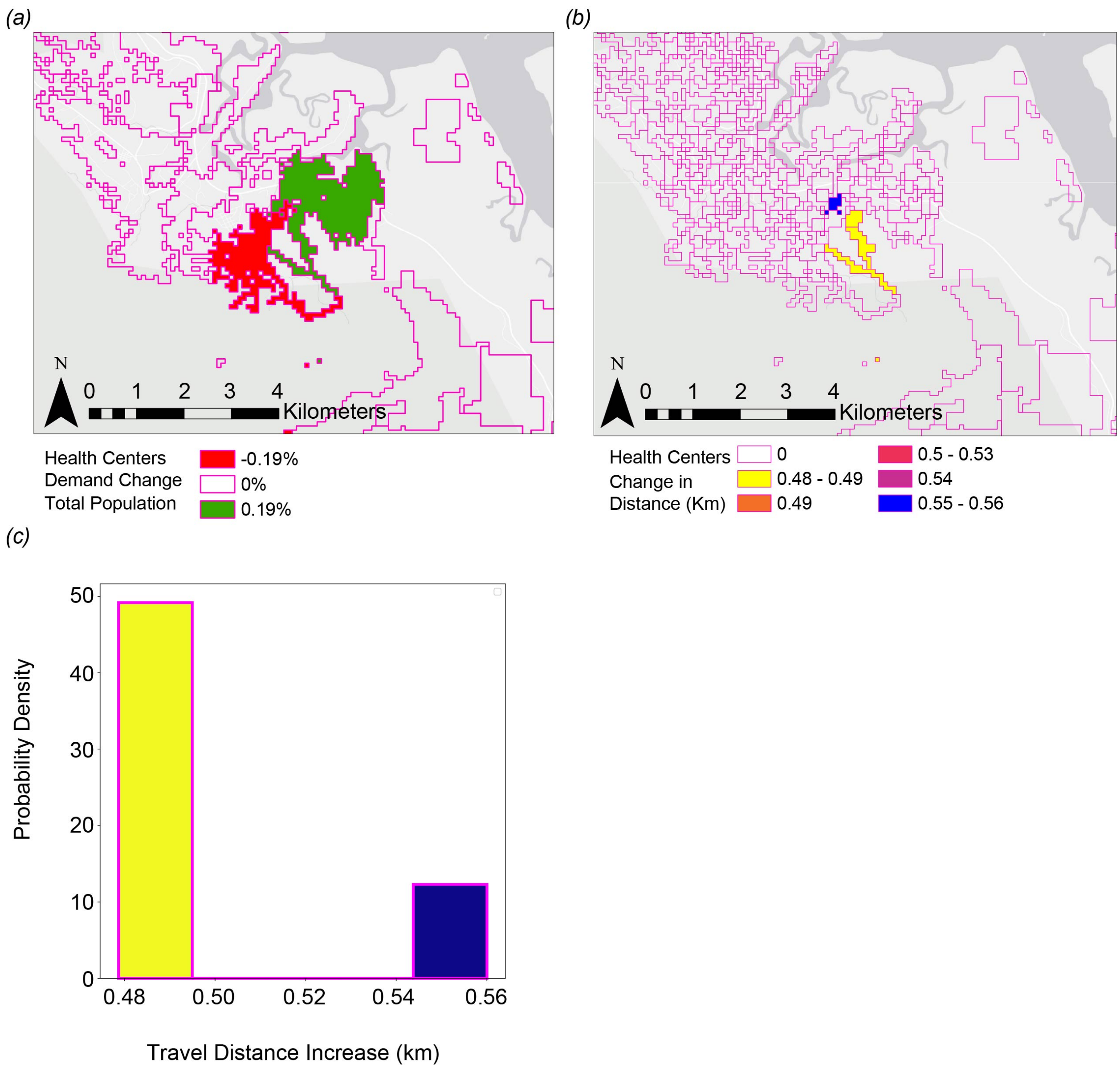

FIGURE A.22: Scenario 1 Results: a) Demand shifts for affected Health Centers; b) Health Center accessibility shifts for affected neighborhoods; c) Distribution of Health Centers accessibility shifts for affected neighborhoods

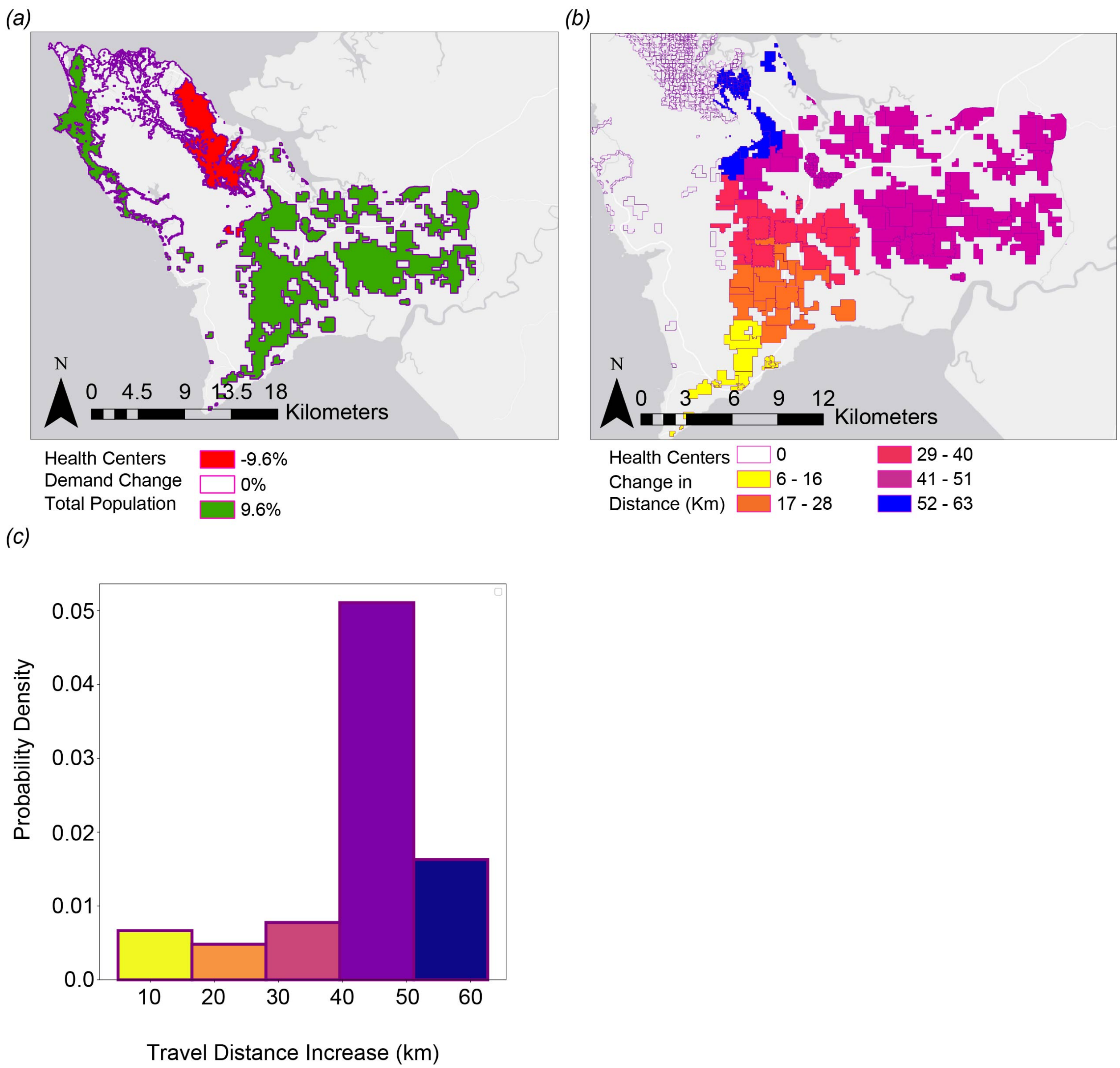

FIGURE A.23: Scenario 1 Results: a) Demand shifts for affected Pharmacies; b) Pharmacy accessibility shifts for affected neighborhoods; c) Distribution of Pharmacies accessibility shifts for affected neighborhoods

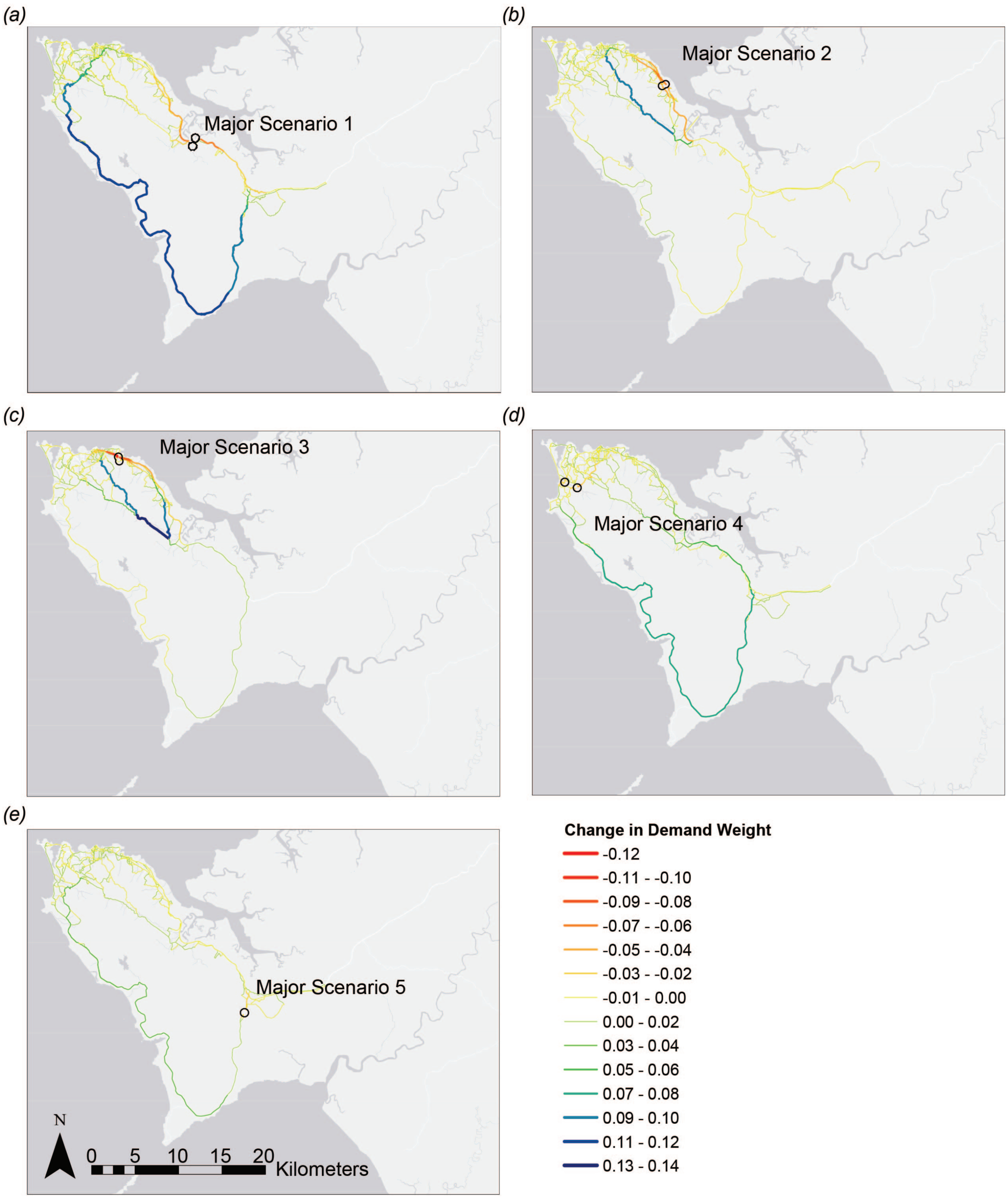

FIGURE A.24: Major Flooding Scenario Results - Non-zero changes in demand weight for a) Scenario 1, b) Scenario 2, c) Scenario 3, d) Scenario 4, e) Scenario 5

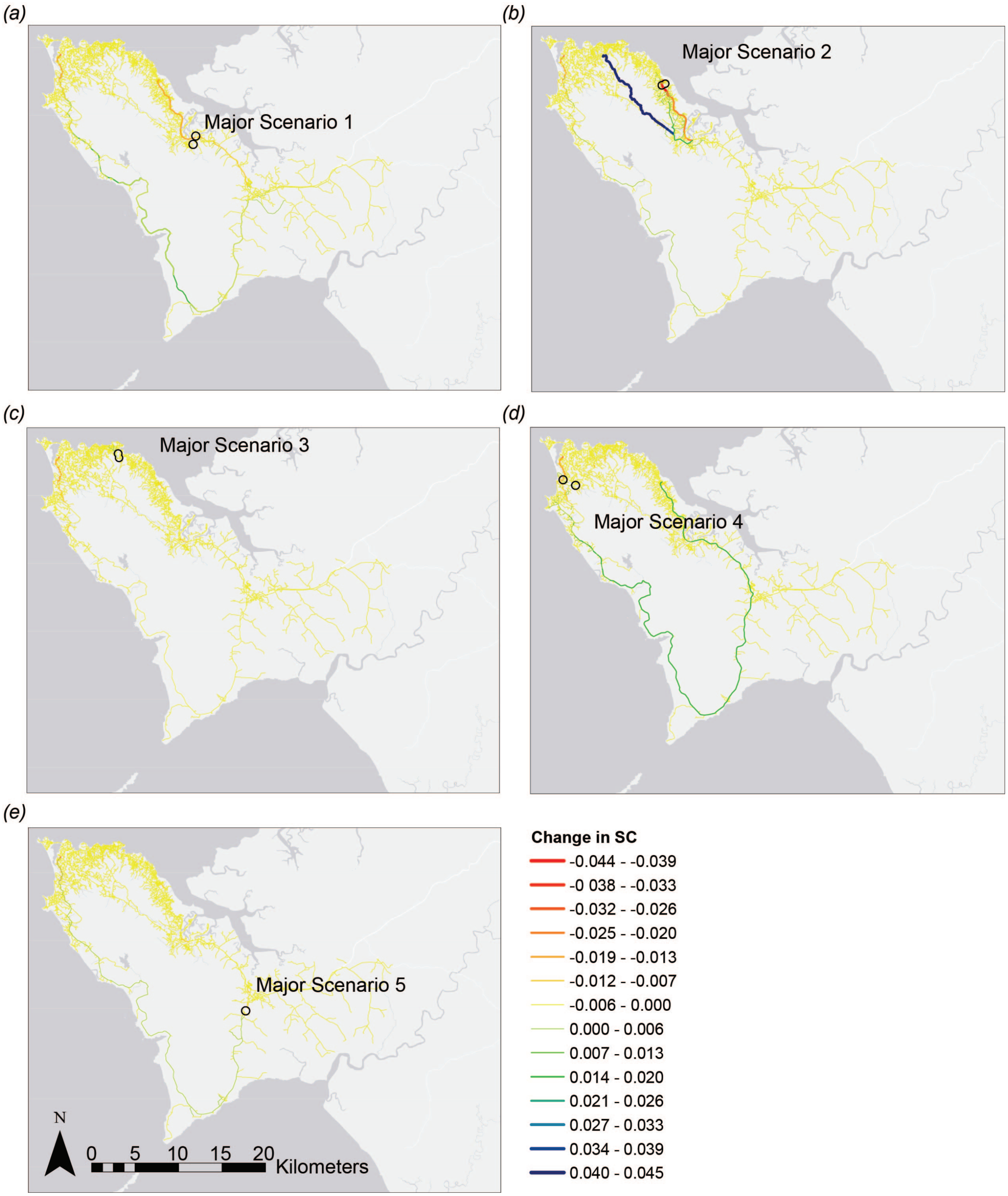

FIGURE A.25: Major Flooding Scenario Results - Non-zero changes in SC for a) Scenario 1, b) Scenario 2, c) Scenario 3, d) Scenario 4, e) Scenario 5

Bibliography

Ackerman, Cameron T (2009). "HEC-GeoRAS–GIS tools for support of HEC-RAS using ArcGIS, User's manual". In: *US Army Corps of Engineers–Hydrologic Engineering Center (HEC)* 4.

Altshuler, Yaniv et al. (2015). "On the rationality and optimality of transportation networks defense: a network centrality approach". In: *Securing Transportation Systems*, pp. 35–63.

Anderson, James Richard (1976). *A land use and land cover classification system for use with remote sensor data*. Vol. 964. US Government Printing Office.

Aslam, Baber, Faisal Amjad, and Cliff C Zou (2012). "Optimal roadside units placement in urban areas for vehicular networks". In: *2012 IEEE Symposium on Computers and Communications (ISCC)*. IEEE, pp. 000423–000429.

Barabási, Albert-László and Réka Albert (1999). "Emergence of scaling in random networks". In: *science* 286.5439, pp. 509–512.

Barthélemy, Marc (2014). *Spatial networks*. Springer.

Bertolini, Luca, Frank Le Clercq, and Loek Kapoen (2005). "Sustainable accessibility: a conceptual framework to integrate transport and land use plan-making. Two test-applications in the Netherlands and a reflection on the way forward". In: *Transport policy* 12.3, pp. 207–220.

Bigotte, João F et al. (2010). "Integrated modeling of urban hierarchy and transportation network planning". In: *Transportation Research Part A: Policy and Practice* 44.7, pp. 506–522.

Brandes, Ulrik et al. (2013). "What is network science?" In: *Network science* 1.1, pp. 1–15.

Brockmann, Dirk, Lars Hufnagel, and Theo Geisel (2006). "The scaling laws of human travel". In: *Nature* 439.7075, p. 462.

Buhl, J et al. (2006). "Topological patterns in street networks of self-organized urban settlements". In: *The European Physical Journal B-Condensed Matter and Complex Systems* 49.4, pp. 513–522.

Cardillo, Alessio et al. (2006). "Structural properties of planar graphs of urban street patterns". In: *Physical Review E* 73.6, p. 066107.

Chen, Anthony et al. (2007). "Network-based accessibility measures for vulnerability analysis of degradable transportation networks". In: *Networks and Spatial Economics* 7.3, pp. 241–256.

Cheng, Jianquan et al. (2013). "Understanding urban networks: Comparing a node-, a density-and an accessibility-based view". In: *Cities* 31, pp. 165–176.

Chowell, Gerardo et al. (2003). "Scaling laws for the movement of people between locations in a large city". In: *Physical Review E* 68.6, p. 066102.

Comber, Alexis, Chris Brunsdon, and Edmund Green (2008). "Using a GIS-based network analysis to determine urban greenspace accessibility for different ethnic and religious groups". In: *Landscape and Urban Planning* 86.1, pp. 103–114.

Cronshey, Roger (1986). *Urban hydrology for small watersheds*. Tech. rep. US Dept. of Agriculture, Soil Conservation Service, Engineering Division.

Cui, Tingting, Yanfeng Ouyang, and Zuo-Jun Max Shen (2010). "Reliable facility location design under the risk of disruptions". In: *Operations research* 58.4-part-1, pp. 998–1011.

Dogan, Ibrahim (2012). "Analysis of facility location model using Bayesian Networks". In: *Expert systems with applications* 39.1, pp. 1092–1104.

Farahani, Reza Zanjirani and Masoud Hekmatfar (2009). *Facility location: concepts, models, algorithms and case studies*. Springer.

Gao, Jian, Yi-Cheng Zhang, and Tao Zhou (2019). "Computational socioeconomics". In: *Physics Reports*.

Gil, Jorge (2015). "Building a multimodal urban network model using openstreetmap data for the analysis of sustainable accessibility". In: *OpenStreetMap in GIScience*. Springer, pp. 229–251.

Gonzalez, Marta C, Cesar A Hidalgo, and Albert-Laszlo Barabasi (2008). "Understanding individual human mobility patterns". In: *nature* 453.7196, p. 779.

Graham, Stephen (2012). "Disrupted cities: infrastructure disruptions as the Achilles heel of urbanized societies". In: *DISASTER, INFRASTRUCTURE AND SOCIETY: Learning from the 2011 Earthquake in Japan=* —— 3, pp. 12–26.

IBRD/The World Bank (2015). *Republic of Ghana: Ghana Work program (FY15) Poverty and Inequality Profile*. URL: `http://documents.worldbank.org/curated/en/258711468255281103/pdf/Ghana-Poverty-profile-final-2.pdf`.

İcaga, Yilmaz, Emin Tas, and Murat Kilit (2016). "Flood inundation mapping by GIS and a hydraulic model (HEC RAS): A case study of Akarcay Bolvadin subbasin, in Turkey". In: *Acta Geobalcanica* 2.2, pp. 111–118.

Kalapala, Vamsi et al. (2006). "Scale invariance in road networks". In: *Physical Review E* 73.2, p. 026130.

Kaluza, Pablo et al. (2010). "The complex network of global cargo ship movements". In: *Journal of the Royal Society Interface* 7.48, pp. 1093–1103.

Keck, Markus and Patrick Sakdapolrak (2013). "What is social resilience? Lessons learned and ways forward". In: *Erdkunde*, pp. 5–19.

Keeling, Matt J and Ken TD Eames (2005). "Networks and epidemic models". In: *Journal of the Royal Society Interface* 2.4, pp. 295–307.

Khalfallah, C Ben and S Saidi (2018). "Spatiotemporal floodplain mapping and prediction using HEC-RAS-GIS tools: Case of the Mejerda river, Tunisia". In: *Journal of African Earth Sciences* 142, pp. 44–51.

Klose, Andreas and Andreas Drexl (2005). "Facility location models for distribution system design". In: *European journal of operational research* 162.1, pp. 4–29.

Kurant, Maciej and Patrick Thiran (2006). "Extraction and analysis of traffic and topologies of transportation networks". In: *Physical Review E* 74.3, p. 036114.

Kute, Sunil et al. (2014). "Flood modeling of River Godavari using HEC-RAS". In: *Int J Res Eng Technol* 3.09, pp. 81–87.

Labbé, Martine, Dominique Peeters, and Jacques-François Thisse (1995). "Location on networks". In: *Handbooks in operations research and management science* 8, pp. 551–624.

Latty, Tanya et al. (2011). "Structure and formation of ant transportation networks". In: *Journal of The Royal Society Interface* 8.62, pp. 1298–1306.

Liu, Suxia and Xuan Zhu (2004). "Accessibility analyst: an integrated GIS tool for accessibility analysis in urban transportation planning". In: *Environment and Planning B: Planning and Design* 31.1, pp. 105–124.

Marcelin, Jean Michael et al. (2016). "How does accessibility to post-disaster relief compare between the aging and the general population? A spatial network optimization analysis of hurricane relief facility locations". In: *International journal of disaster risk reduction* 15, pp. 61–72.

Melkote, Sanjay and Mark S Daskin (2001). "An integrated model of facility location and transportation network design". In: *Transportation Research Part A: Policy and Practice* 35.6, pp. 515–538.

Merwade, Venkatesh (2012a). "Terrain processing and HMS-model development using GeoHMS". In: *Lafayette, Indiana*.

— (2012b). "Watershed and stream network delineation using ArcHydro Tools". In: *University of Purdue, School of Civil Engineering, Printed Lecture Note, USA*.

Montis, A et al. (2007). "Structure of inter-cities traffic: a weighted network analysis". In: *Environ. Plan.* 34.

NASA/METI/AIST/Japan Spacesystems (2009). *ASTER Global Digital Elevation Model [Internet]. NASA EOSDIS Land Processes DAAC*. Available from `https://lpdaac.usgs.gov/products/astgtmv002/`.

Nelson, Andrew et al. (2019). "Coupling Natural Hazard Estimates with Road Network Analysis to Assess Vulnerability and Risk: Case Study of Freetown, Building Disruption Simulations in Hydrometeorological Risk Areas in Data-Scarce Sierra Leone". In: *Transportation Research Record*, p. 0361198118822272.

OpenStreetMap (2015). *Planet dump [Data file from 1 Febuary 2019]*. Retrieved from `https://planet.openstreetmap.org`.

Pelling, Mark et al. (2004). "Reducing disaster risk: a challenge for development". In:

Puzis, Rami et al. (2013). "Augmented betweenness centrality for environmentally aware traffic monitoring in transportation networks". In: *Journal of Intelligent Transportation Systems* 17.1, pp. 91–105.

Rosenzweig, Cynthia et al. (2018). *Climate change and cities: Second assessment report of the urban climate change research network*. Cambridge University Press.

Salman, F Sibel and Eda Yücel (2015). "Emergency facility location under random network damage: Insights from the Istanbul case". In: *Computers & Operations Research* 62, pp. 266–281.

Serede, Imbenzi J, Benedict M Mutua, and James M Raude (2014). "A review for hydraulic analysis of irrigation canals using HEC-RAS model: a case study of Mwea irrigation scheme, Kenya". In: *Hydrology* 2.1, pp. 1–5.

Statistics Sierra Leone (2016). "Sierra Leone 2015 population and housing census". In: *Provisional Results. Freetown Sierra Leone: Statistics Sierra Leone*.

Taylor, Michael AP and GM D'este (2003). "Concepts of network vulnerability and applications to the identification of critical elements of transport infrastructure". In: New Zealand Transport Research Forum Wellington, New Zealand.

Taylor, Michael AP, Somenahalli VC Sekhar, and Glen M D'Este (2006). "Application of accessibility based methods for vulnerability analysis of strategic road networks". In: *Networks and Spatial Economics* 6.3-4, pp. 267–291.

World Bank (2018). *Sierra Leone Multi-City Hazard Review and Risk Assessment : Technical Methodology and Summary of Results : Final Report (English)*. URL: `http://documents.worldbank.org/curated/en/821161549318730387/Technical-Methodology-and-Summary-of-Results-Final-Report`.

World Bank Group (2018). *Republic of Sierra Leone Priorities for Sustainable Growth and Poverty Reduction : Systematic Country Diagnostic*. URL: `https://openknowledge.worldbank.org/handle/10986/29701`.

WorldPop (2013). *Sierra Leone 100m Population [Internet]. University of Southampton; 2013. Alpha version 2010 and 2014 estimates of numbers of people per grid square, with national totals adjusted to match UN population division estimates (http://esa.un.org/wpp/)*. Available from: `http://www.worldpop.org.uk/data/summary/?doi=10.5258/SOTON/WP00234`.

Zhang, Tong et al. (2016). "Examining the amenability of urban street networks for locating facilities". In: *Physica A: Statistical Mechanics and its Applications* 457, pp. 469–479.

Zobler, L (1999). "Global soil types, 1-degree grid (zobler)". In: *ORNL DAAC*.